Chapter 3

RESULTS

Study Part I: Osteogenic induction of rat bone marrow

1. Bone marrow cell cultur

1.1. Attachment and growth of bone marrow

Bone marrow of fully mature rats, 10 months-old, were induced and differentiated to express phenotypes of osteoblasts in cell culture. At an initial loading, most of the cells have a round shape with different sizes mixing with a large numbers of blood cells. At 12 hours after seeding, stromal cells started to attach on the surface of the culture plate while blood cells floated in the culture medium. During 48 - 72 hours after seeding, initial morphological change of attaching cells could be seen. Cells spread their cytoplasms on flat surface and started to form cell nodules. Numbers and size of cell nodules increased with the culture time resulting from an increase in size and numbers of cells. Cells reached confluence at around the 12^{th}-14^{th} culture-days.

Morphologies of differentiated bone marrow cells varied. Predominantly, they were fibroblast-like cells having a round nucleus with elongated cytoplasm and round shaped cells with foamy cytoplasm. Morphologies of cells in the first passage are more homogenous of fibroblast-like cells. Cells reached confluence at around the 12^{th}-14^{th} culture-day (Figure 3- 1).

1.2. Factors influencing attachment and growth of bone marrow cells during 72 hours after seeding of bone marrow

1. It was observed that density of the initial cell seeding was an important factor determining growth of cells. Cells with low seeding density grew slowly.
2. Mechanical injury during single cell preparation had a significant effect to cell death and detachment of cells from the culture surface 72 hours after seeding.
3. Forty-eight hours after cell seeding cells should be continuously incubated in 5% CO_2 at 37°C with a minimum disturbance. Culture medium should be changed at 48 – 72 hours after seeding.
4. TGF-β2 at 5 ng/ml in a culture medium had different effects on morphological change of attaching cells compared to morphological changes of cells cultured in dexamethasone or BMP-2. It seemed to promote differentiation of cells to fibroblast-like cells and reduce formation of cell nodules.

Figure 3- 1 Bone marrow cell culture supplemented with 20 nM dexamethasone in primary passage

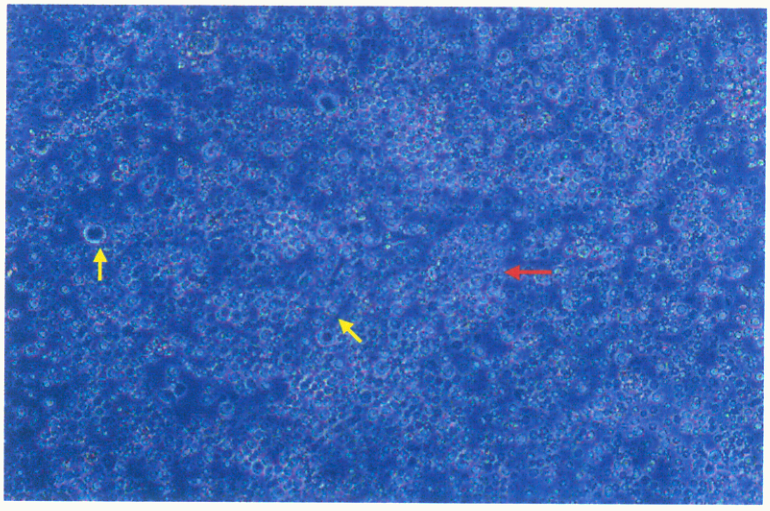

(a) At 24-48 hours after cell seeding, observing an initial cell attachment (↑) and floating of blood cells (↑) (40 x 10 x 10)

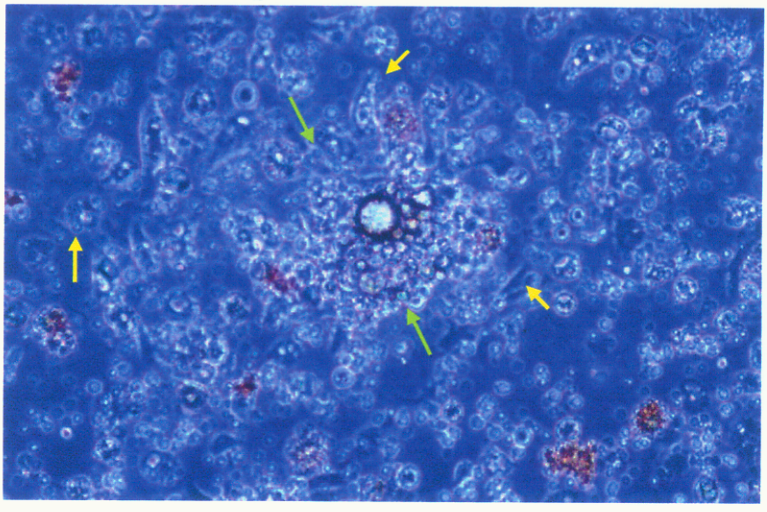

(b) At 72 hours after cell seeding, observing early cell nodule formation (↑) and initial morphological differentiation with various shapes of cells (↑) (x 400)

Figure 3-1 (continue): Bone marrow cell culture supplemented with 20 nM dexamethasone in primary passage

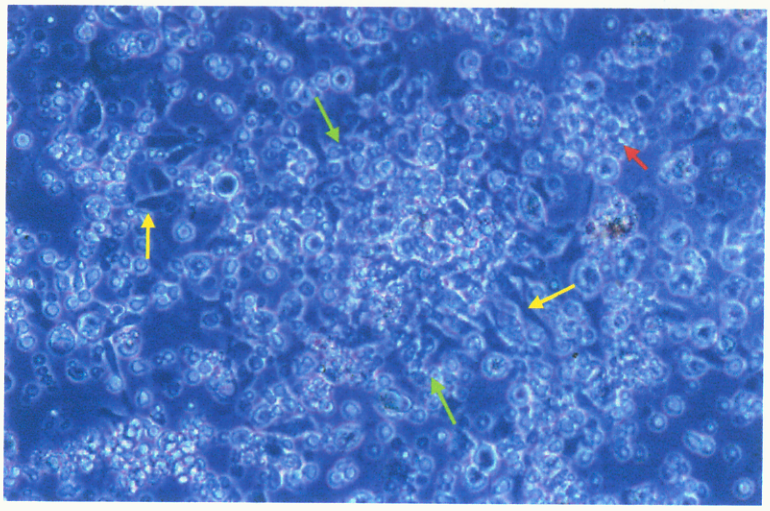

(c) At the 4^{th} – 5^{th} culture-day observing an increasing number of small size fibroblast-like cells, with elongated cytoplasm (↑), residual blood cells (↑) and a larger size cell nodule (↑) (x 400)

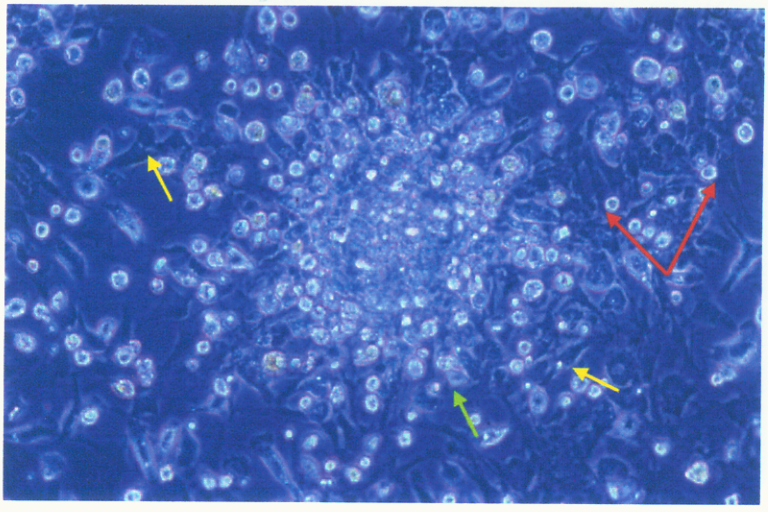

(d) At the 9^{th} 10^{th} culture-day observing a lager numbers and size of fibroblast-like cells, a larger size cell nodule and remnant of blood cells (x 400)

Figure 3-1 (continue): Bone marrow cell culture supplemented with 20 nM dexamethasone in primary passage

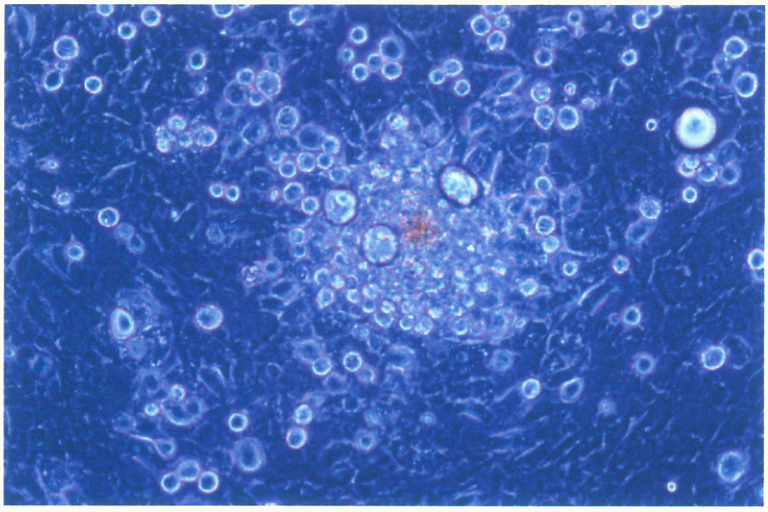

(e) At the 13^{th} – 14^{th} culture-day, observing a contact between cells creating a monolayer of cell culture (x 400).

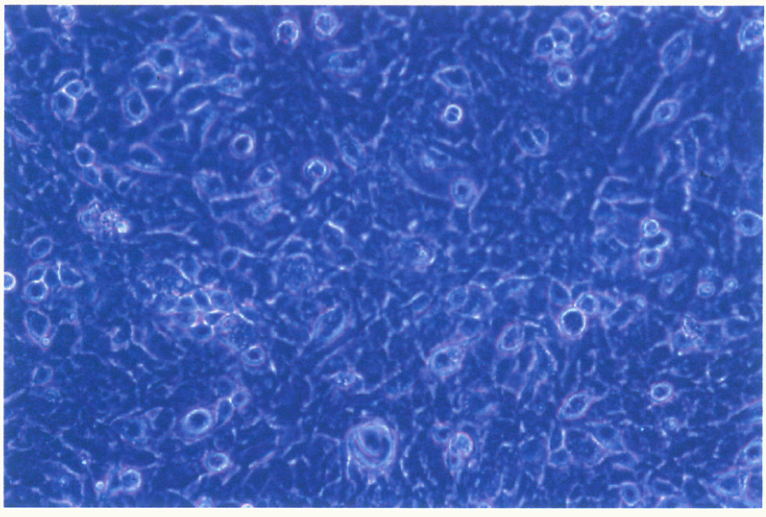

(f) At the 19^{th} – 20^{th} culture-day observing dense multi-cell layers (x 400)

2. Identifying adipocytic and chondroblastic differentiations

2.1. Adipocytes

Adipocytes were found as early as 48 hours after cell seeding. Oil red O staining demonstrates red lipid droplets within cytoplasm. They were found throughout cell culture in primary and first passages. Adipocytes grew well in cell culture of poor cell growth. They located surrounding cell nodules mixing with fibroblast-like cells (Figure 3-2)

2.2. Chondroblasts

Positive staining of Alcian blue in cytoplasm was not found. A light blue staining of Alcian blue staining was found in the extracellular matix (ECM) at the middle of the cell nodules and between cells (Figure 3-3).

Figure 3- 2: Adipocytes with Oil red O staining of lipid droplets within cytoplasm

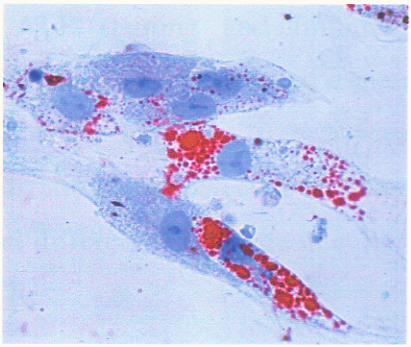

(a) Adipocytes in cell culture of normal growth (x 600)

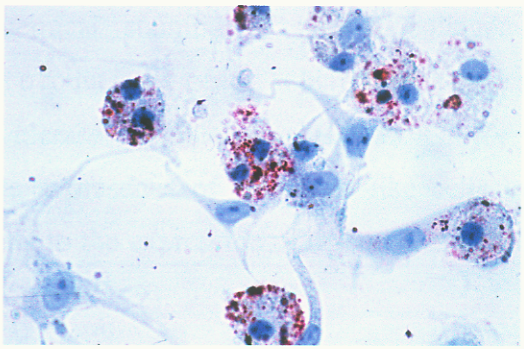

(b) Adipocytes in in poor cell culture (x 400)

Figure 3- 3: Alcian blue staining of extracellular matrix

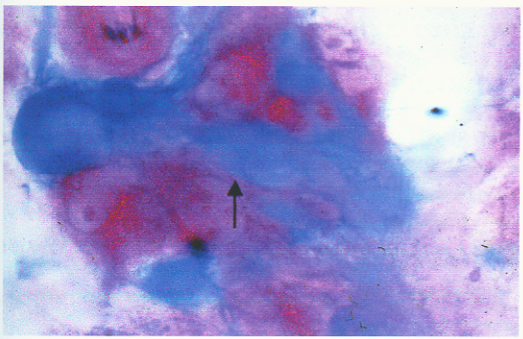

(a) Light blue staining of ECM of cell nodule (↑) of cell nodule (a) and between cells (↑) (x 600)

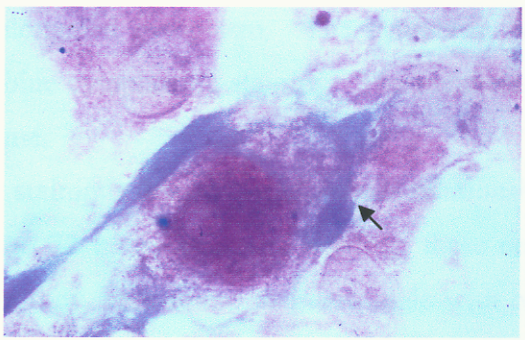

(b) Light blue staining of ECM between cells (x 600)

3. Identifying osteoblast-like cells

ALP staining and Immunohistochemical staining of type I collagen and osteocalcin were performed to demonstrate products of genes, where their expressions were found in a reverse transcriptase polymerase chain reaction (RT-PCR). *In vitro* mineralization was detected to demonstrate a presence of osteoblast-like cells in the terminal differentiation stage in corresponding to the expression of osteocalcin mRNA in RT-PCR.

3.1. ALP staining

Positive staining of ALP was found as early as at 48 hours after cell seeding. At this stage, positive stained cells were still looking like clumps of cells. At 72 hours, positive staining in cytoplasm of elongated cells was seen. At the 5 culture-day, positive stained cells are fibroblast-like cells with elongated cytoplasm. The cytoplasm was positively stained with various intensities of blue cytoplasmic staining. The numbers of positive stained cells increased with culture-time.

Double staining of oil red O and ALP stainings demonstrated a close relationship between these two types of cells. During the 72 hours after cell seeding, these cells located in the same clump of cells. Later on they were found to intermingle with one another surrounding cell nodules. At the 14^{th} culture-day, most of the cells were fibroblast-like cells with an ALP positive stain (Figure 3-4).

3.2. Immunohistochemical stainings of collagen type I and osteocalcin

Positive staining of type I collagen was found at the 7^{th}, 14^{th} and 21^{st} culture-days in primary and first passages of all groups. Fine brownish red staining was found in the cytoplasm and ECM. Staining of ECM was more obvious when cells reached confluence and became multi-layers (Figure 3-5a).

Positive staining of osteocalcin was found only in cell cultures with 50 nM rhBMP-2 at the 14^{th} and 21^{st} culture-days and 10 nM VD3 at the 21^{st} culture-day in

primary and first passages. It was a fine brownish-red staining in cytoplasm (Figure 3-5b).

3.3. *In vitro* mineralization, von Kossa staining

Positive staining of von Kossa stain was found in all twelve representative samples (3 samples per group) of cell cultures at the 21st culture-day of Groups B (BMP-2) and C (VD3) in primary and first passages. A mild positive staining was found in only one in three samples of Group A (Dexamethasone). Dark staining in the middle of the cell nodules was interpreted as a positive stain (Figure 3-6).

Figure 3- 4: Double staining of ALP and Oil red O stainings of bone marrow cells cultivated in 20 nM dexamethasone

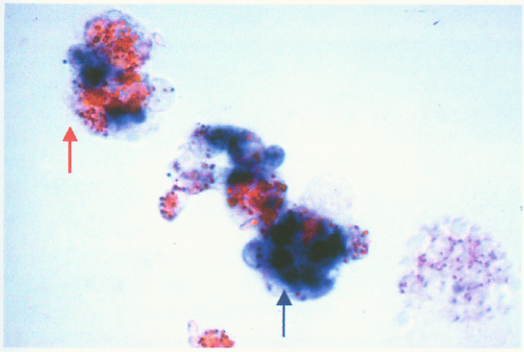

(a) Co-positive stainings of oil red O, red lipid droplets (↑) and ALP, blue cytoplasmic staining (↑), in primary passage at 48 hours after cell seeding (x 400)

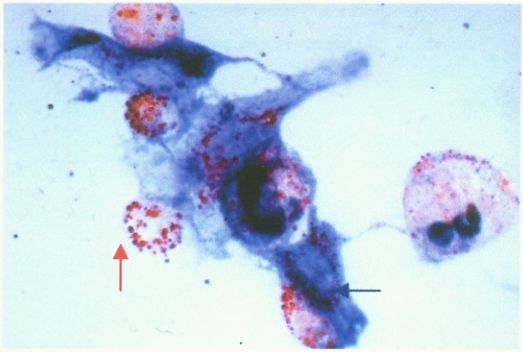

(b) A co-positive staining at 72 hours after cell seeding (x 400)

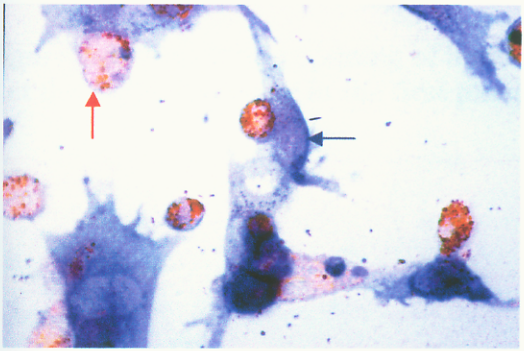

(c) An advance morphological differentiation of osteoblast-like (↑) and fat cells (↑) from bone marrow cells at 5 days after cell seeding (x 400)

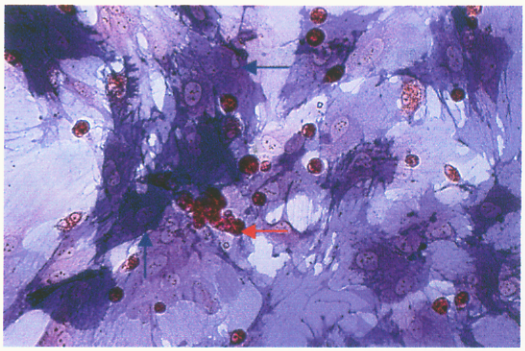

(d) At the 14th culture-day or at an initial confluence in the first passage observing a mixing of osteoblast-like cells (↑) and a few fat cells (↑) (x 400)

Figure 3- 5 Immunohistochemical staining of type I collagen and osteocalcin of bone marrow cell culture at the 14 culture-day in the first passage

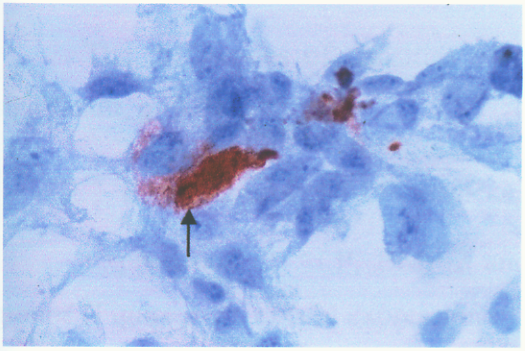

(a) Type I collagen – brownish-red staining (↑) in ECM of bone marrow cells cultivated in 20 nM dexamethasone (x 400)

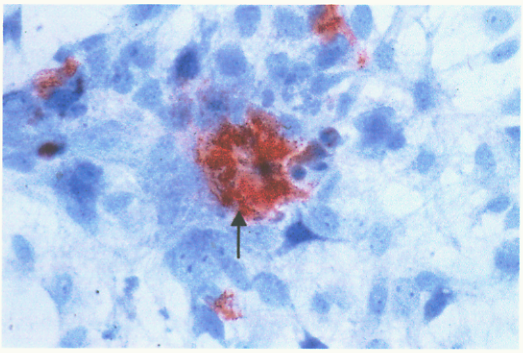

(b) Osteocalcin – brownish-red staining (↑) in ECM of bone marrow cells cultivated in 50 ng/ml rhBMP-2 (x 400)

Figure 3- 6 Von Kossa staining of bone marrow cells cultivated in 50 ng/ml rhBMP-2 at the 21st culture-day in the first passage

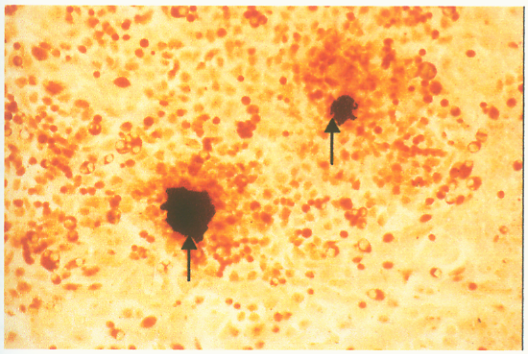

(a) Various size of black staining at center of cell nodules (x 200)

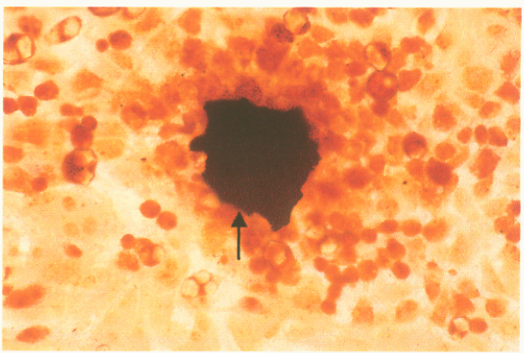

(b) Mineralization of ECM in cell nodule (x400)

4. Expressions of mRNAs of bone marrow cells of fully mature rats, 11 month-old, cultivated in 10 nM VD3 and 50 ng/ml rhBMP-2

4.1. Reliability control

The differences of densities of each band from three measurements were not significant, $p>0.05$.

4.2. Expressions of ALP, BMP-2, Type I Collagen and osteocalcin mRNAs

Expressions of ALP, BMP-2 and Type I collagen mRNAs were found in all groups (Figure 3-8), except expression of osteocalcin mRNA was found only in Group B (VD3) and Group C (BMP-2). Levels of mRNA expression in Group C was stronger than the expression in Group B (Figure 3-8).

In Group A (Dexamethasone), expressions of ALP and BMP-2 had been found through out the cell culture period since the 7^{th} culture-day in the primary passage. Expression of Type I collagen was found as early as the 14^{th} culture-day in each passage. Expression of osteocalcin mRNA was not found in this group (Figure 3-9).

In Group B (VD3), expression of type I collagen was first found at the 14^{th} culture-day. Expression of osteocalcin mRNA was found at the 21^{st} culture-day in primary passage and since the 7^{th} culture-day in the first passage. Expressions of ALP and BMP-2 were found through-out the cell culture period (Figure 3-10).

In Group C (BMP-2), expression of type I collagen was found earlier than in the other two groups. It had been found since the 7 culture-day in the primary and first passage. Similarly to Group B (VD3), expression of osteocalcin was found at the 21^{st} culture-day in the primary passage and since the 7^{th} culture-day in the first passage. It could be observed that expressions of ALP and BMP-2 mRNAs were consistently high through-out the cell culture period (Figure 3-11).

Figure 3- 7 Gel electrophoresis of RT-PCR products of bone marrow cells in first passage at the 13th culture-day cultivated in 20 nM Dexamethasone (Group A)

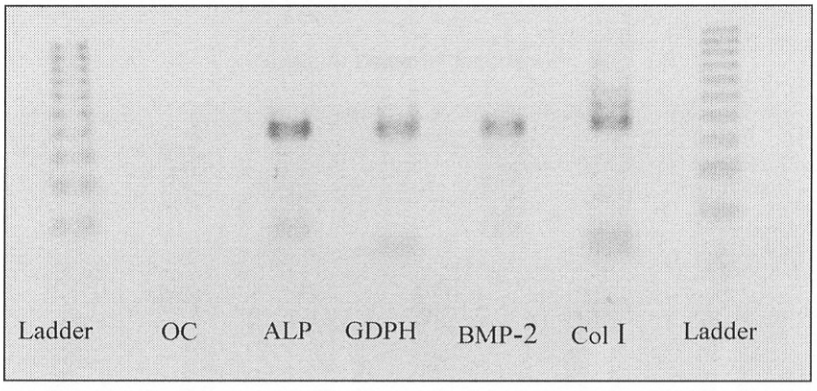

(Ladder = base pair marker, OC = osteocalcin, ALP = alkaline phosphatase, GDPH = house keeping gene, BMP-2 = BMP-2, Col I = type I collagen)

Figure 3- 8 Gel electrophoresis of bone marrow cells in first passage at the 14th culture-day cultivated in VD3 (Group B) (a) and BMP-2 (Group C) (b)

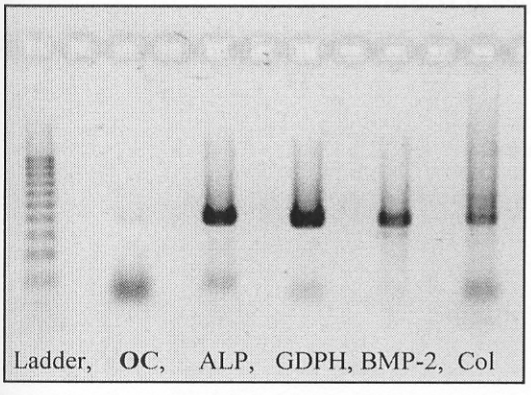

(a) Group B: VD3

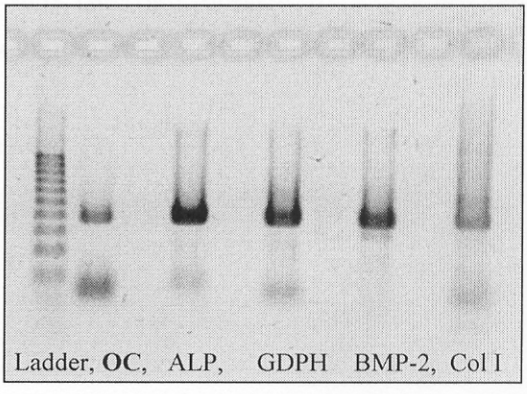

(b) Group C: BMP-2

Demonstrating differences of intensity and size of positive bands of osteocalcin mRNA

(Ladder = base pair marker, OC = osteocalcin, ALP = alkaline phosphatase, GDPH = house keeping gene, BMP-2 = BMP-2, Col I = type I collagen)

Figure 3- 9 Group A:Dexamethasone bone marrow cell culture in primary and first passages

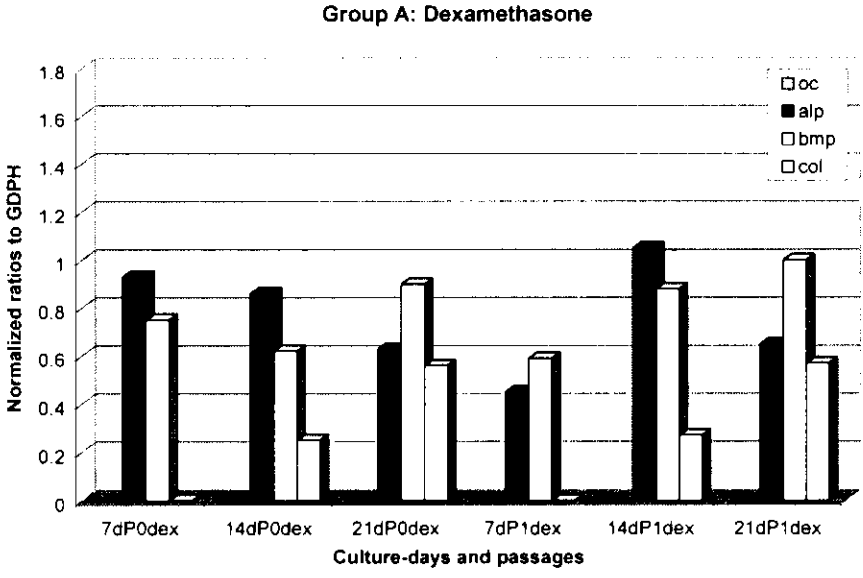

(d = culture-day, P = culture passage, 0 = primary, 1 = first, dex = Group A:Dexamethasone, oc = osteocalcin, alp=ALP, bmp=BMP-2, col=type I collagen)

Figure 3- 10 Group B:VD3 bone marrow cell culture in primary and first passages

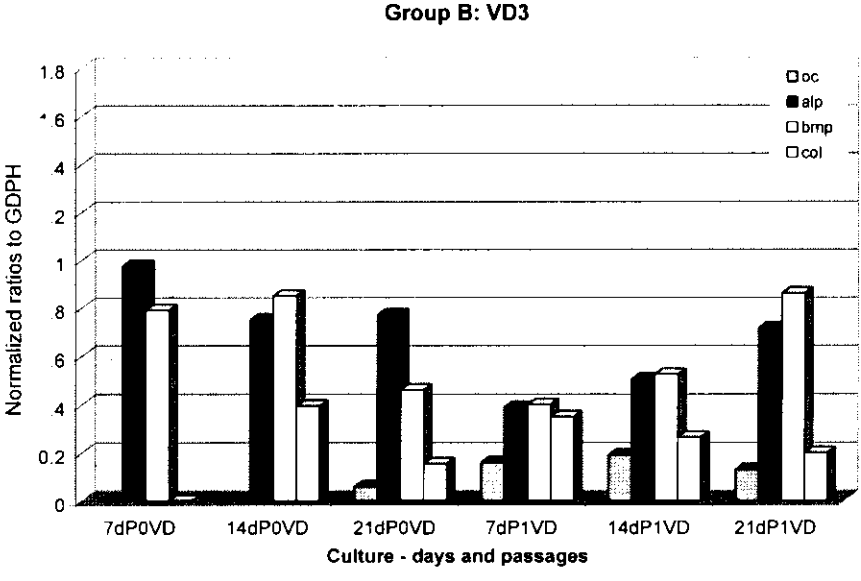

(d = culture-day, P = culture passage, 0 = primary, 1 = first, VD = Group B:VD3, oc = osteocalcin, alp=ALP, bmp=BMP-2, col=type I collagen)

Figure 3- 11 Group C:BMP-2, bone marrow cell culture in primary and first passages

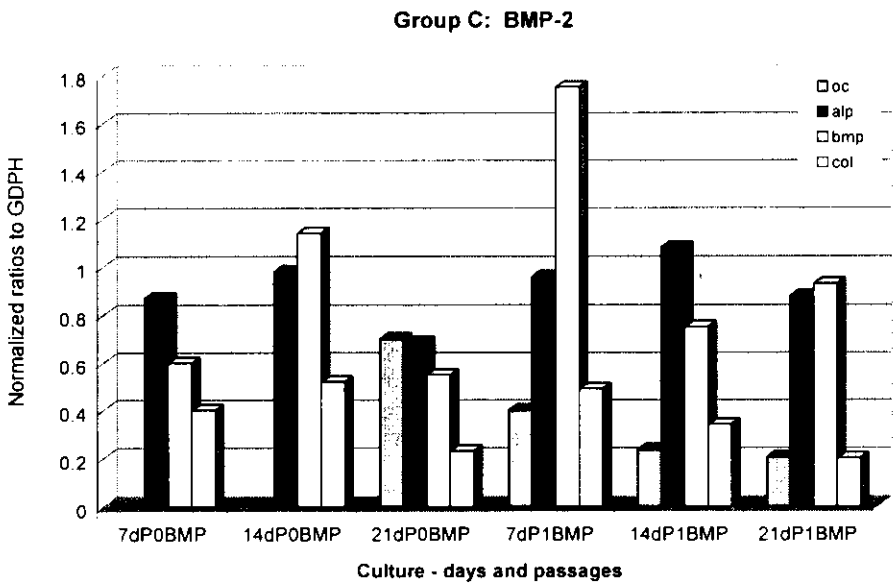

(d = culture-day, P = culture passage, 0 = primary, 1 = first, BMP = Group C:BMP-2, oc = osteocalcin, alp=ALP, bmp=BMP-2, col=type I collagen)

5. An implantation of fresh bone marrow and differentiated bone marrow cells in nude mice

A total of 22 ICBM scaffolds were implanted into 12 mice. One specimen was lost because of local infection. All mice survived the operation and were sacrificed at 6, 18, 28 and 45 days. New bone formation was found in all matrixes loaded with fresh or cultivated bone marrow cells as early as the 18th implantation-day. The amount of bone formation from implanted fresh bone marrow was minimal.

5.1. Implanted cells

Cultivated bone marrow cells seeded on 18 scaffolds were a mixture of at least two types of cells. Most of them were pre-mature osteoblast-like cells demonstrated by positive staining of ALP staining, which were mixed with a few adipocytes demonstrated by positive staining of oil red O (Figure 3-12).

5.2. Radiographs

Small mineralization foci were first seen in radiograph at implantation-day 6 (Figure 3-13). The amount and density of the radiopaque mass was markedly demonstrated at the 18th culture-day (Figure 3-14). The differences in radiographic images of implanted scpecimens at implantation-days 28 and 45 were not obviously different. On the 28th and 45th implantation-day, the area and density of the mineralization area were clearly higher than what was found in the radiographs of implantation-day 18 specimens (Figure 3-15 and Figure 3-16). A small mineralization area was found in the radiographs of implanted fresh bone marrow at implantation-day 45 (Figure 3-17).

Figure 3- 12 Alkaline phosphatase and Oil red O stainings of implanted cells in nude mice

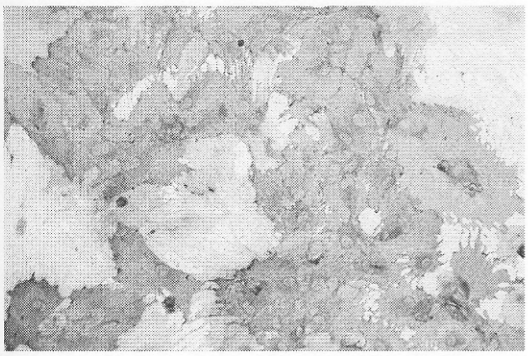

(a) ALP staining (x 400)

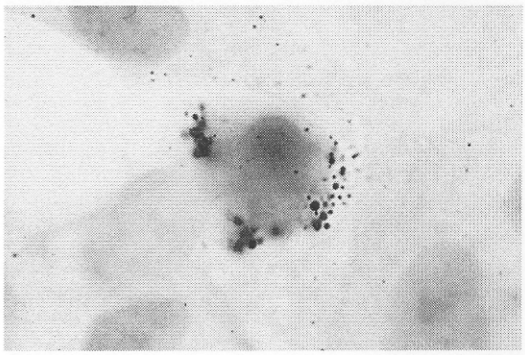

(b) Oil red O staining (x 400)

Figure 3- 13 Radiographs of cultivated bone marrow on ICBM scaffold at 6th implantation-day

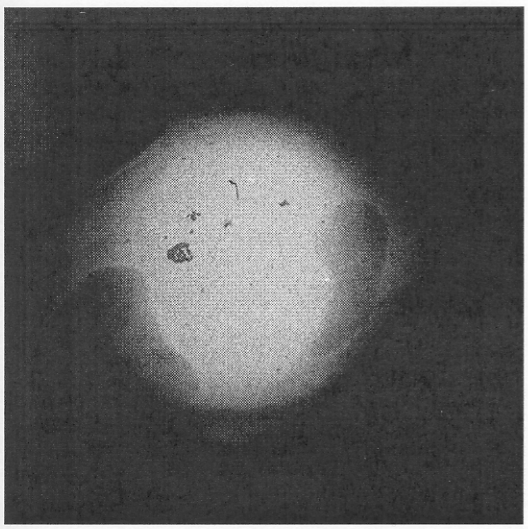

(a) No evidence of mineralization

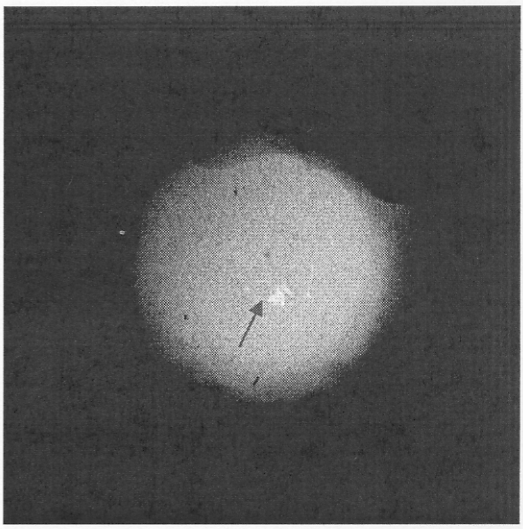

(b) Observing small radiopaque foci (↑) in one sample

Figure 3- 14 Radiographs of Group B: Cultivated bone marrow on ICBM scaffold at implantation-day 18

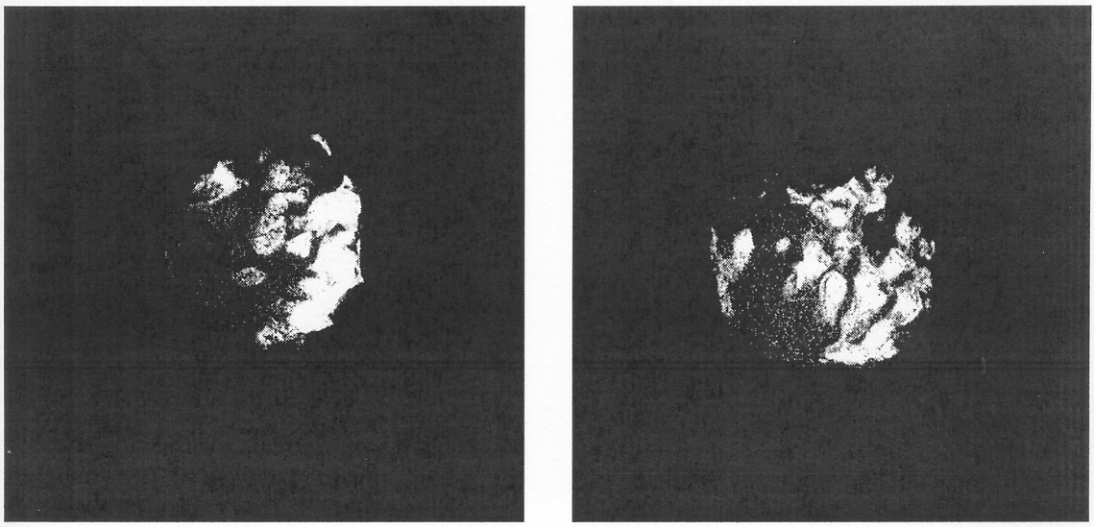

Figure 3- 15 Radiographs of Group B: cultivated bone marrow on ICBM scaffold at implantation-day 28

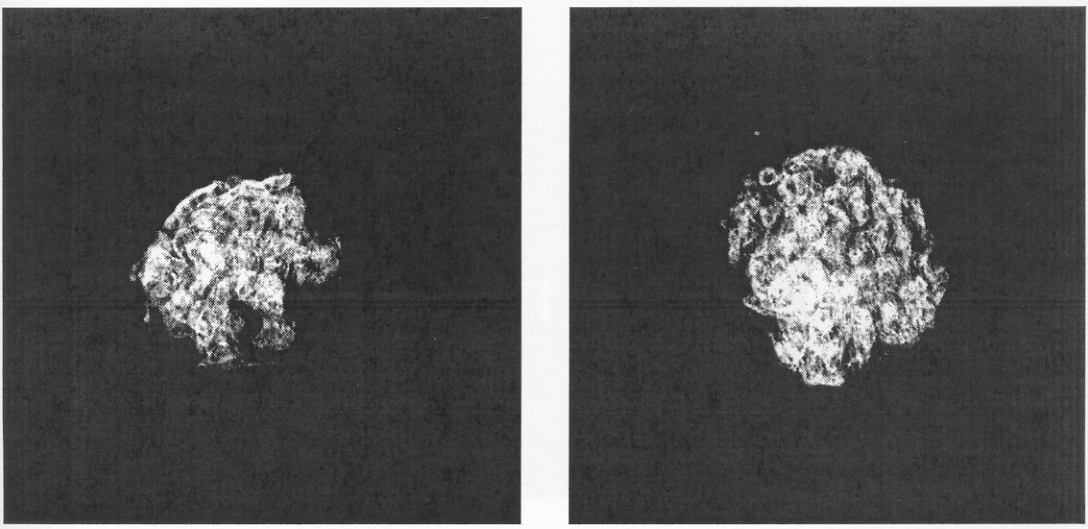

Figure 3- 16 Radiographs of Group B: Cultivated bone marrow on ICBM scaffold at implantation-day 45

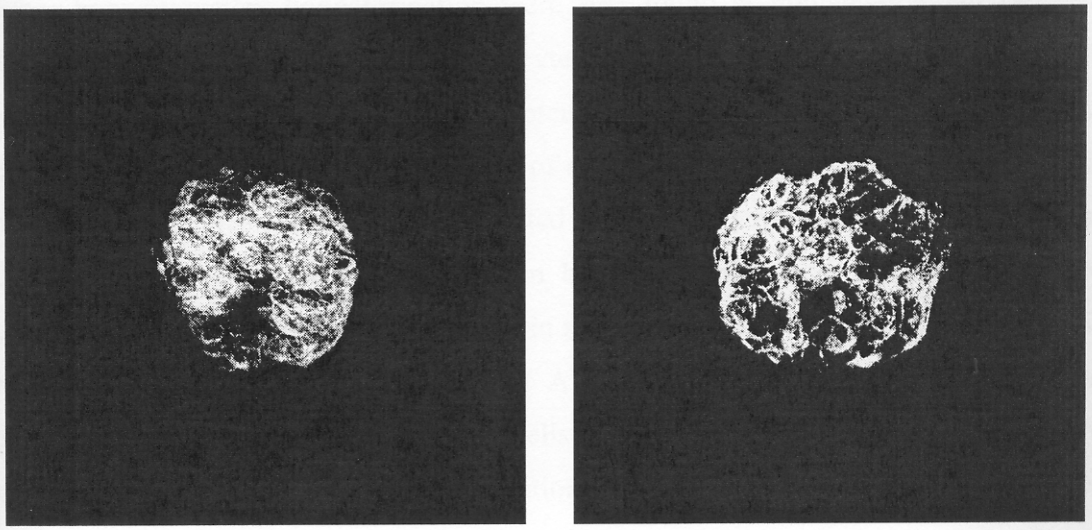

Figure 3- 17 Radiographs of Group A: Fresh bone marrow on ICBM scaffold at implantation-day 45

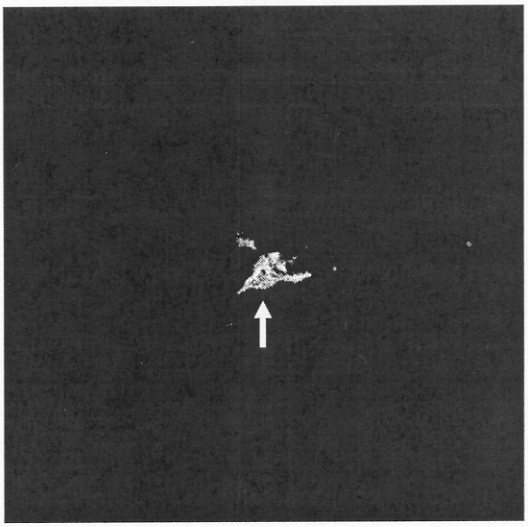

(a) Observing small radiopaque foci (↑) in one sample

5.3. Histology

Foci of woven bone formation were first found at implantation-day 18. The osteogenesis center of osteoblasts, osteocytes and differentiated hyperchromatic cells were found within the pore space. Bone spicules were laid down mainly within the pore of the scaffold and directly on the surface of scaffold in some areas. Bone formation in the mature stage was markedly demonstrated in implanted specimens from the 28th and 45th implantation-days, which was woven bone with no evidence of lamellar bone formation. Cartilage formation was found in some areas. The bone formation process in fresh bone marrow implantation (Group A) was slower than the process of bone formation in implantation of cultivated cells (Group B). The structure of the ICBM scaffold was still intact at the 45 implantation day. No evidence of scaffold resorption and inflammatory reaction was found. There was no evidence of new bone formation or mineralization in Group C (ICBM scaffold only).

5.3.1. At 6 implantation-day

5.3.1.1. Group B: ICBM scaffold with bone marrow cells in first passage

At implantation-day 6, accumulation of dense connective tissue was found in peripheral pores of the ICBM scaffold. The central area of the ICBM scaffold was filled with loose connective tissue. In an area of dense connective tissue aggregation of undifferentiated mesenchymal cells, hyperchromatic cuboidal-shape cells, and fibroblast-like cells were found. Pink collagenous scaffold was found in-between fibroblast-like cells and in ECM (Figure 3-18).

5.3.2. At implantation-day 18

5.3.2.1. Group B: ICBM scaffold and bone marrow cells in first passage

At implantation-day 18 new bone formation was in an early stage. Undifferentiated mesenchymal cells, dense connective tissue and hyperchromatic

cuboidal shaped cells were found within the pores of ICBM scaffolds. Large osteoblasts were embedded in unorganized bone scaffolds lined or surrounded by cuboidal-hyperchromatic cells or osteoblasts. Bone formation was confined in the pores of the ICBM scaffold in the peripheral area. Blood vessels invaded into the bone formation area (Figure 3-19 and Figure 3-20). An area of cartilage formation was found. Mature chondrocytes with large nuclei in lacunae were found surrounded by proliferative chondrocytes and connective tissue stroma (Figure 3-21).

5.3.2.2. Group A: ICBM scaffold and fresh bone marrow

In a group of implanted fresh bone marrow (Group A) no mineralization was found. Within the pore of the scaffold, dense connective tissue and vessels were accumulated within the space. Bands of hyperchromatic cuboidal shaped cells and pink collagenous tissue were found surrounding connective tissue stroma next to the surface of the scaffold. No foci of bone formation was found (Figure 3-22).

5.3.3. At implantation-day 28

5.3.3.1. Group B: ICBM scaffold with bone marrow cells in first passage

At implantation-day 28, bone formation was in the mature stage. Trabeculae of woven bone were found without osteoblast cell lining. Osteocytes were embedded in smaller lacunae. Differentiated bone marrow, fat cells and blood vessels were found. Bone formation was formed directly on the surface of the ICBM scaffold and in the pore space. In some areas bone trabeculae were surrounded by dense connective tissue stroma composing of cuboidal shaped undifferentiated mesenchymal cells and fibroblast-like cells (Figure 3-23).

5.3.4. At implantation-day 45

5.3.4.1. Group B: ICBM scaffold with bone marrow cells in first passage

At implantation-day 45, most bone formation was in a mature stage without osteoblast cell lining. Osteocytes embedded in bone trabeculae were surrounded by differentiated bone marrow. A bone matrix was laid on the surface and within the pores of ICBM scaffolds. Bone marrow was well developed. Hematopoietic cells, fat cells and blood vessels were clearly presented in the bone marrow. Cartilage was not found in specimens from this implantation-day on (Figure 3-24 a and b). Osteoblast cell lining and differentiated mesenchymal cells were found in few areas (Figure 3-24 c and d).

5.3.4.2. Group A: ICBM scaffold with fresh bone marrow

In this group, cartilage and bone formation were found. A large area of cartilage was found within pores of the scaffolds. Cartilage was directly connected to and surrounded by intramembranous bone with osteocytes in lacunae. Atrophic chondrocytes embedded in a cartilaginous matrix were found in the central part of the cartilage. Bone marrow and blood vessels were seen surrounding the cartilage and bone (a and b). This might demonstrate a replacing process of cartilage by the bone in the endochondral bone formation process.

Trabeculae of mature woven bone with osteocytes embedded in the bone matrix without osteoblast cells lining were also found. Most of the bone matrix was fully mineralized. The trabeculae were surrounded by differentiated bone marrow and blood vessels. Osteoid seam was seen on the peripheral border of the trabeculae. Osteoid and mineralized bone matrix was found surrounding osteocytes forming lacunae (Figure 3-25 c and d).

Figure 3- 18 Implantation of cultivated cells on ICBM scaffold at implantation-day 6

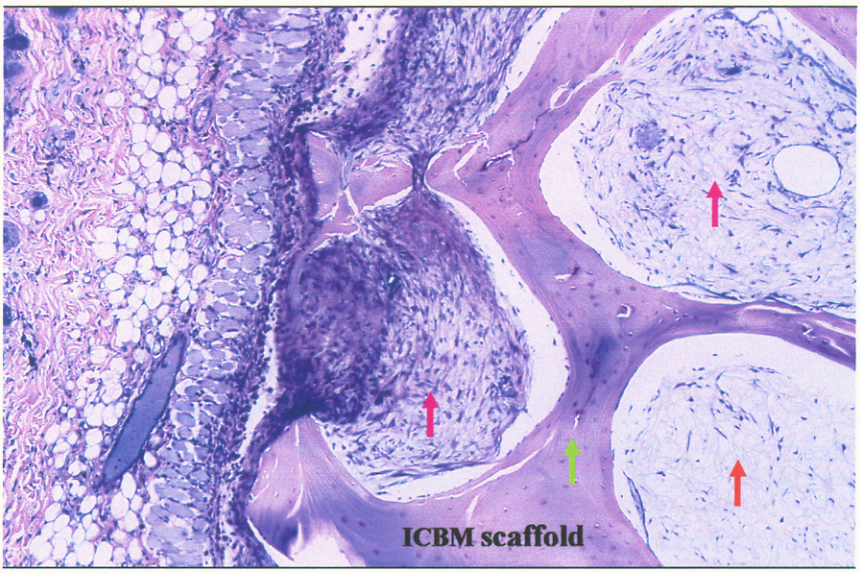

(a) Demonstrating framework of the scaffold, pink trabeculae with empty lacunae (↑), accumulation of dense connective tissue masses on peripheral pores of scaffold (↑) and loose connective tissue within pores of scaffolds (↑), (Giemsa staining, x 200)

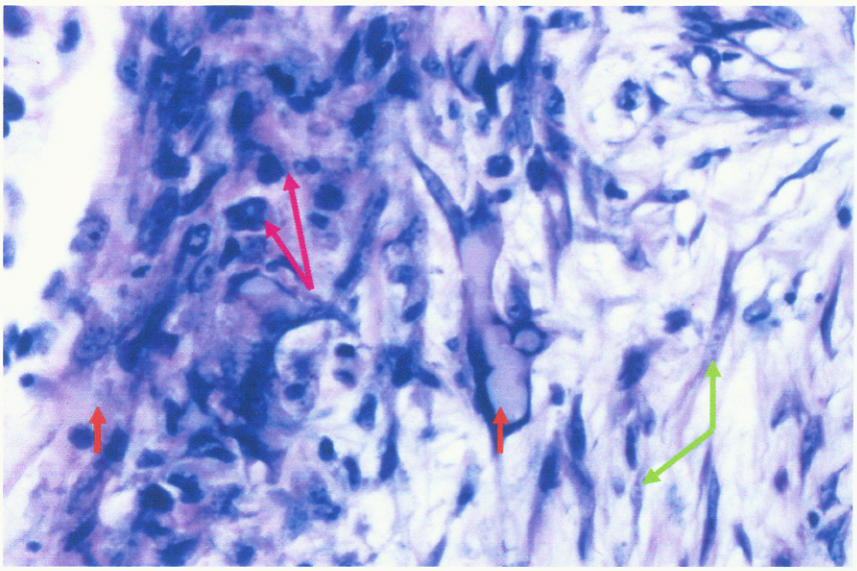

(b) Demonstrating hyperchromatic cuboidal shaped cells (↑), fibroblast-like cells (↑) and collagenous-like tissue in extracellular scaffold (↑) (Giemsa staining 40 x 10 x 1.5)

Figure 3- 19 Implantation of cultivated cells on the ICBM scaffold at implantation-day 18

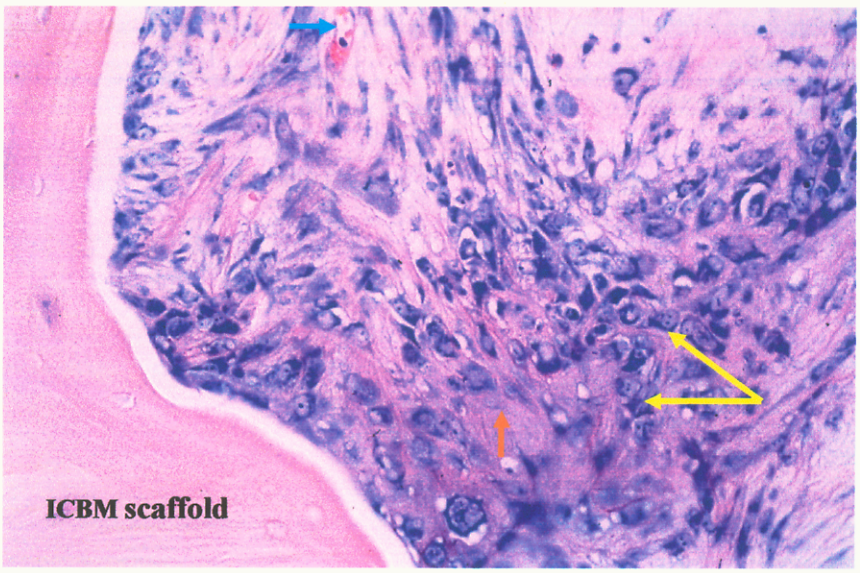

(a) Demonstrating dense hyperchromatic cuboidal cells (↑) embedded in dense connective tissue stroma (↑) within the pore of ICBM scaffold and the invading blood vessel (↑) (Giemsa staining, x 200)

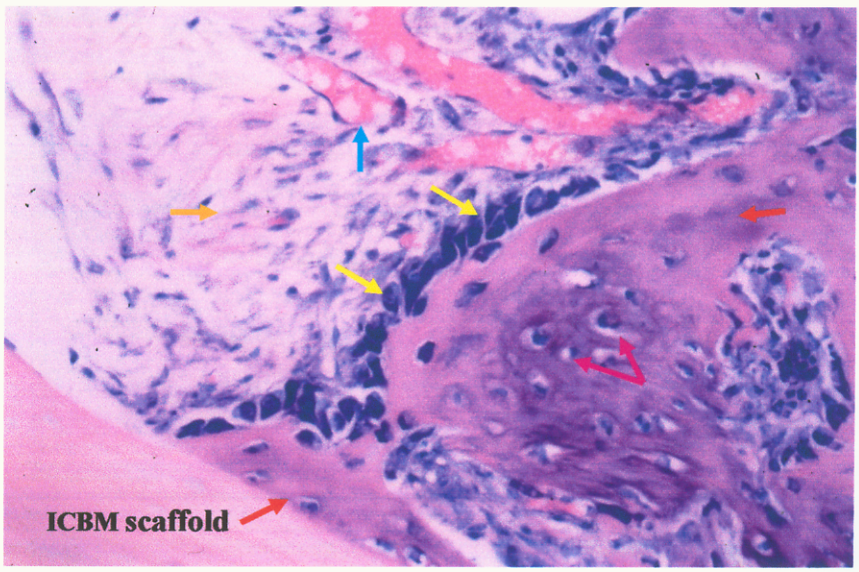

(b) Demonstrating a new woven bone (↑), embedding of osteoblasts in large lacunae (↑), a single layer of osteoblasts cell lining (↑) surrounded by connective tissue stroma (↑) and blood vessels with red blood cells (↑) (Giemsa staining, x 400)

Figure 3- 20 Implantation of cultivated cells on the ICBM scaffold at implantation-day 18

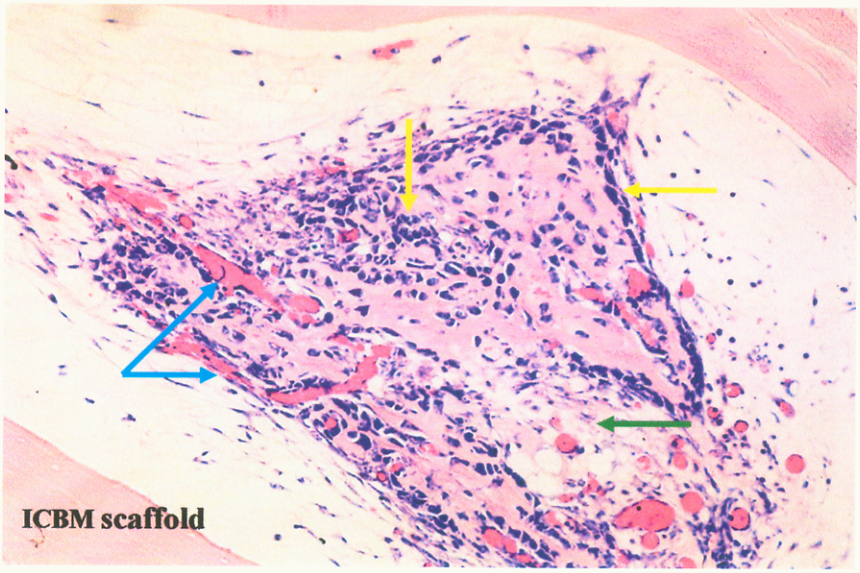

(a) Demonstrating an island of new bone formation surrounded by osteoblasts (↑), blood vessels (↑) and loose connective tissue (↑) within the pore of the scaffold (Giemsa staining x 200)

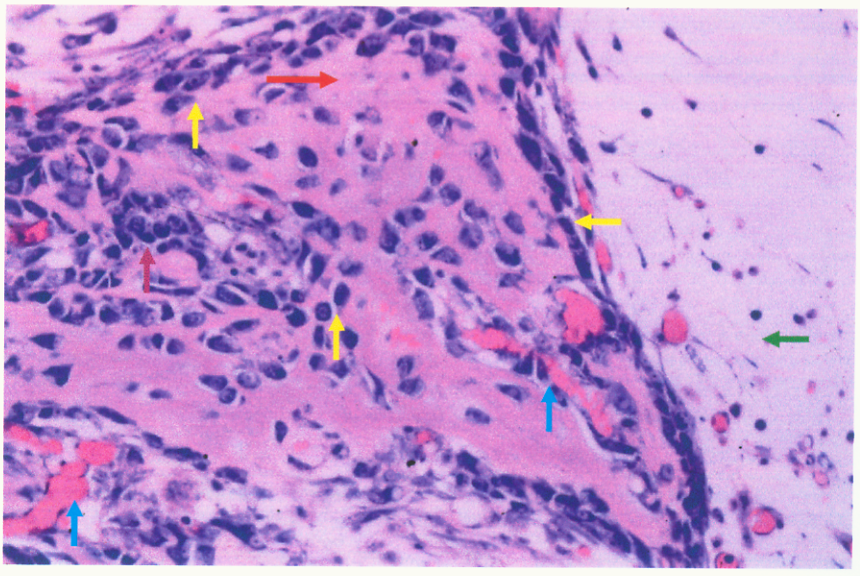

(b) Demonstraing differentiated cuboidal shaped cells (↑), osteoblast lining (↑) unorganized bone matrix (↑), embedding of mature osteoblasts in bone matrix (↑), infiltrating blood vessel (↑) and loose connective tissue (↑) (Giemsa staining, x 400)

Figure 3- 21 Cartilage formation in implantation of cultivated cells on the ICBM scaffold at culture-day 18

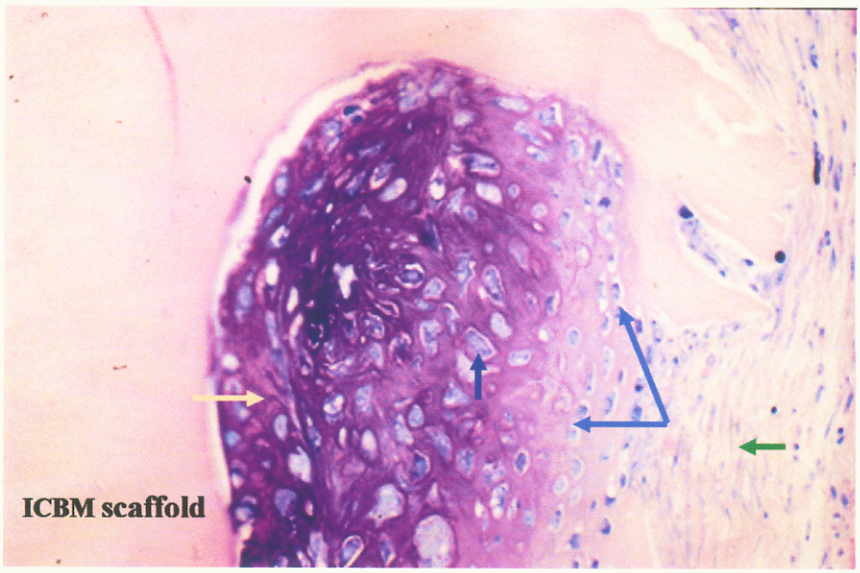

(a) Demonstrating mature chondrocytes (↑) embeded in a cartilagenous matrix ( ) surrounded by a zone of young chondrocytes (↑)and connective tissue stroma (↑) (Giemsa staining, x 200)

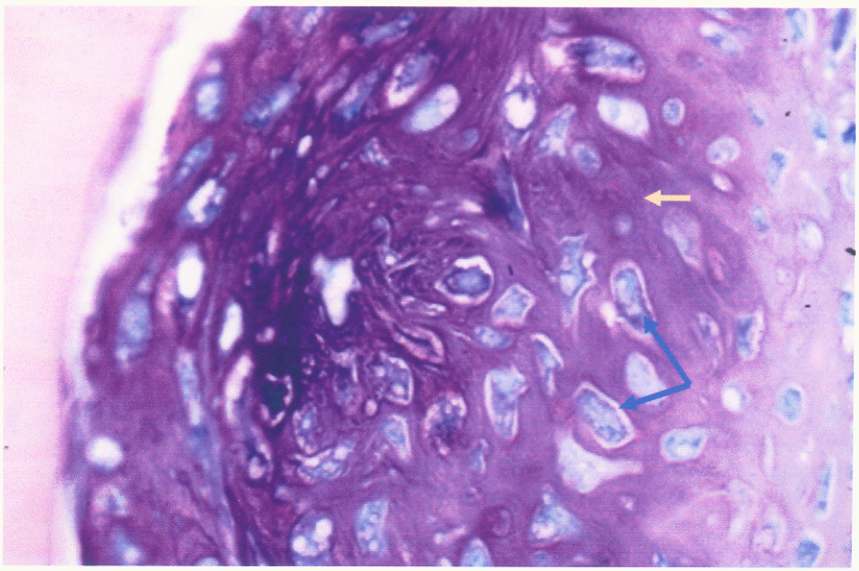

(b) Magnification of mature cartilage observing large mature chondrocytes in lacunae (↑) and cartilaginous matrix ( ) (Giemsa staining, x 800)

Figure 3- 22 Implantation of fresh bone marrow on the ICBM scaffold at implantation-day 18

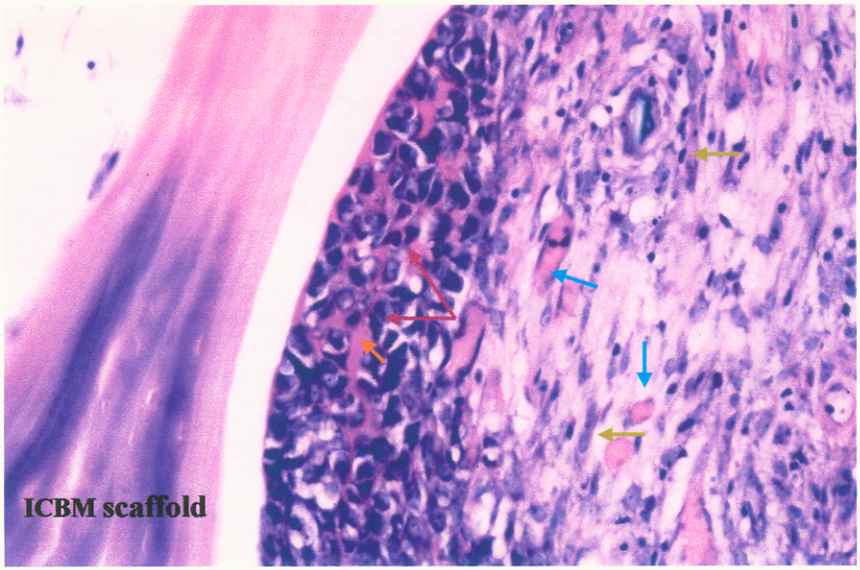

(a) Demonstrating arranging of hyperchromatic cuboidal shaped cells in a band-like form (↑) next to the surface of the ICBM scaffold, fibroblast-like cells (↑), blood vessels (↑) and collagenous extracellular matrix (↑), with no evidence of mineralization (Giemsa staining, x 400)

Figure 3- 23 Implantation of cultivated cells on the ICBM scaffold at implantation-day 28

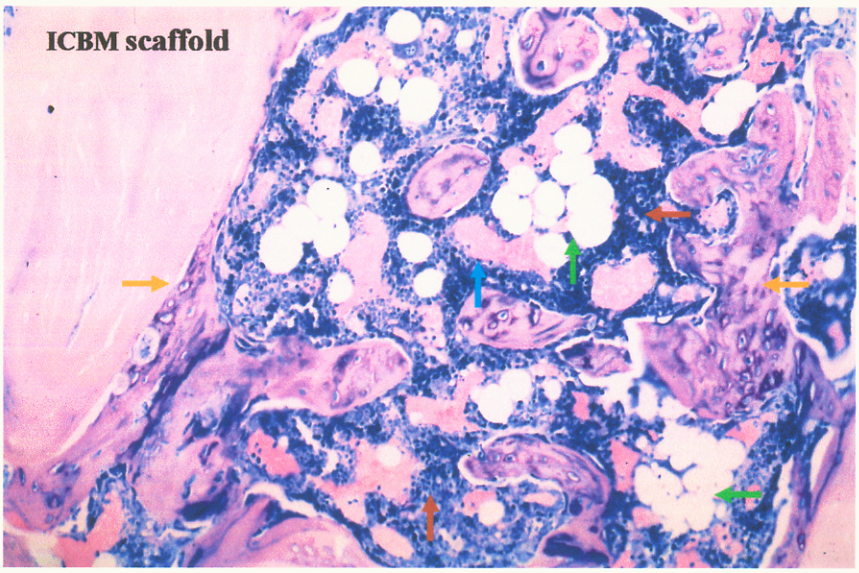

(a) Demonstrating trabeculae of mature woven bone, bone formation in pore and on surface of scaffold (↑), blood vessels (↑) bone marrow cells (↑) and fat tissue (↑)
(Giemsa staining, x 200)

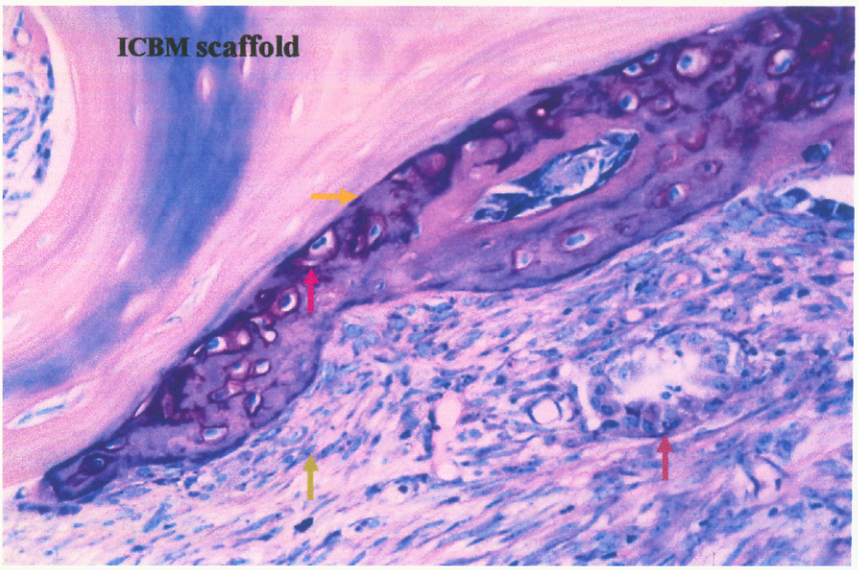

(b) Demonstrating bone formation on the surface of the matrix without osteoblast lining (↑) and embedded of osteocytes in lacunae (↑), undifferentiated mesenchymal cells (↑) and fibroblast-like cells (↑), (Giemsa staining, x 400)

Figure 3- 24 Implantation of cultivated cells on the ICBM scaffold at implantation-day 45

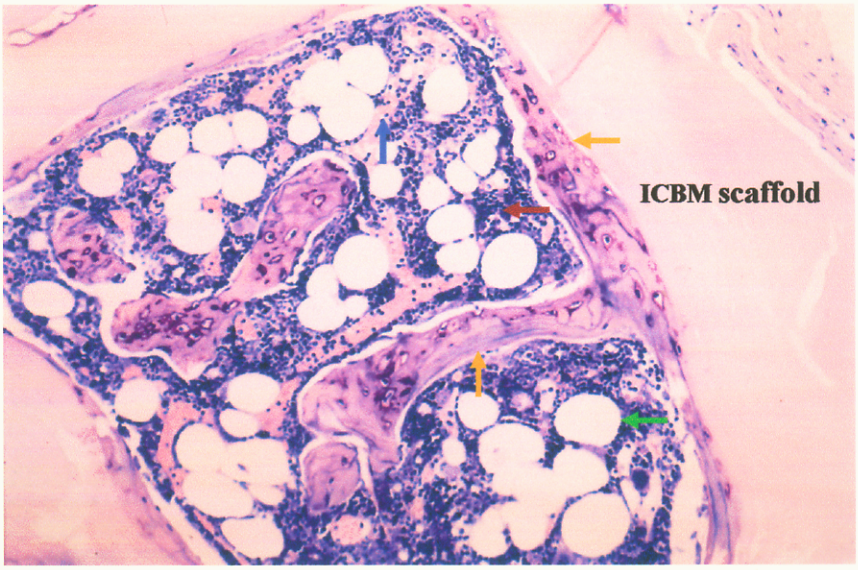

(a) Demonstrating trabeculae of mature woven bone formed on the surface (↑) and within the pore of ICBM scaffold (↑), bone marrow cells (↑), fat tissue (↑) and blood vessels (↑) (Giemsa staining 20 x 10 x1)

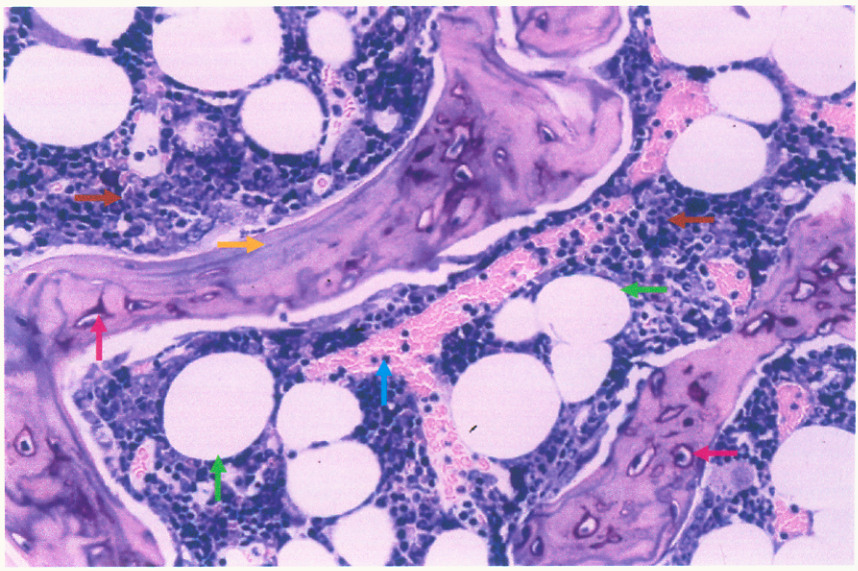

(b) Demonstrating mineralized bone matrix (↑) osteocytes in lacunae (↑),differentiated blood cells (↑), fat tissue (↑) and blood sinusoid with red blood cells (↑) in mature bone marrow (Giemsa staining, x 400)

Figure 3-24 (continuous): Implantation of cultivated cells on the ICBM scaffold at implantation-day 45

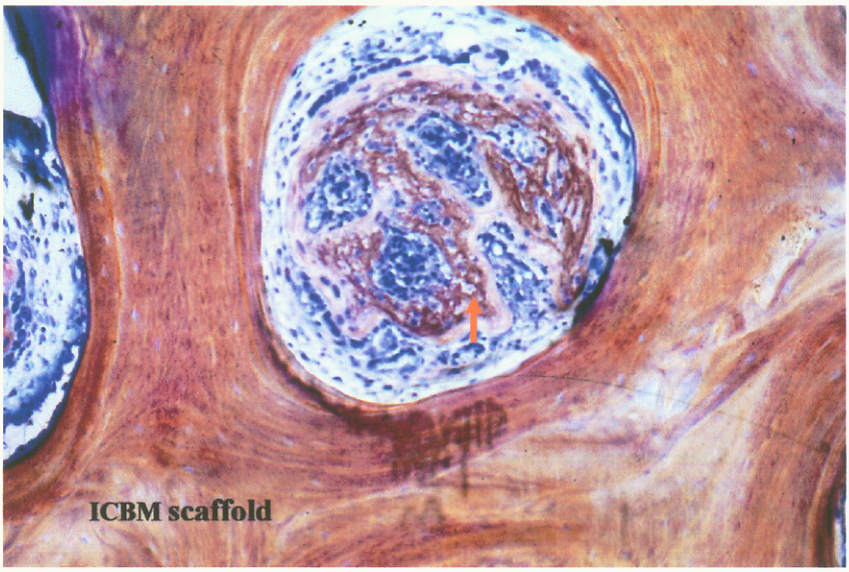

(c) Undecalcified specimen, demonstrating an island of mineralized bone trabeculae (↑) within pore of ICBM matrix (von Kossa and Giemsa double stainings, x 200)

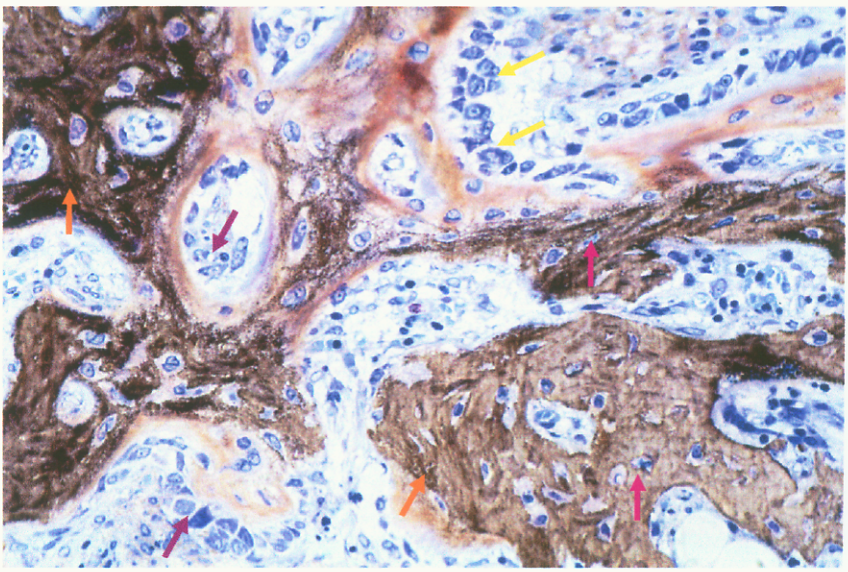

(d) Undecalcified specimen, demonstrating mineralized bone trabeculae with various intensities of brown staining (↑), osteocytes (↑),osteoblast cell lining (↑) and differentiated mesenchymal cells (↑) (von Kossa and Giemsa double stainings, x 400)

Figure 3- 25 Implantation of fresh bone marrow on the ICBM scaffold at implantation-day 45

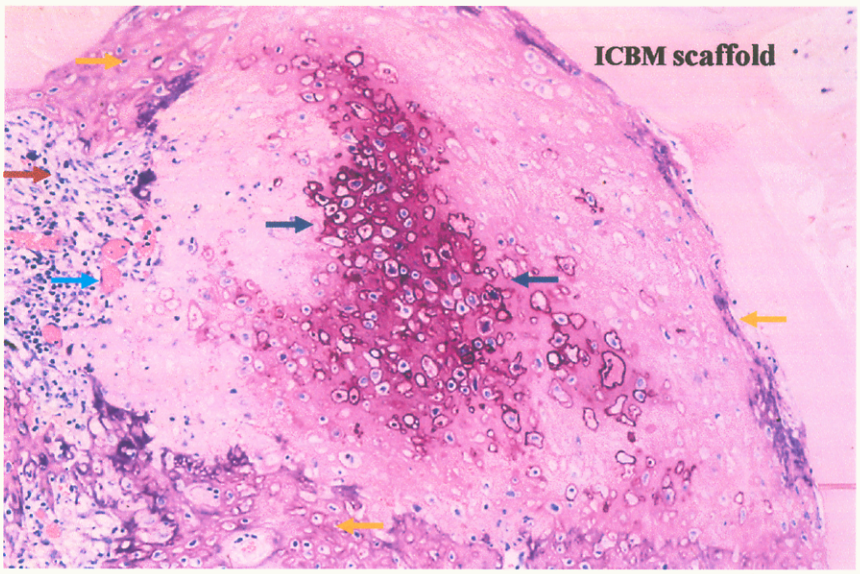

(a) Endochondral bone formation noting aging cartilage with small size chondrocytes at central area of cartilage (↑) and mineralized bone matrix surrounding cartilage (↑), blood vessels (↑) in bone marrow (↑) (Giemsa staining, x 200)

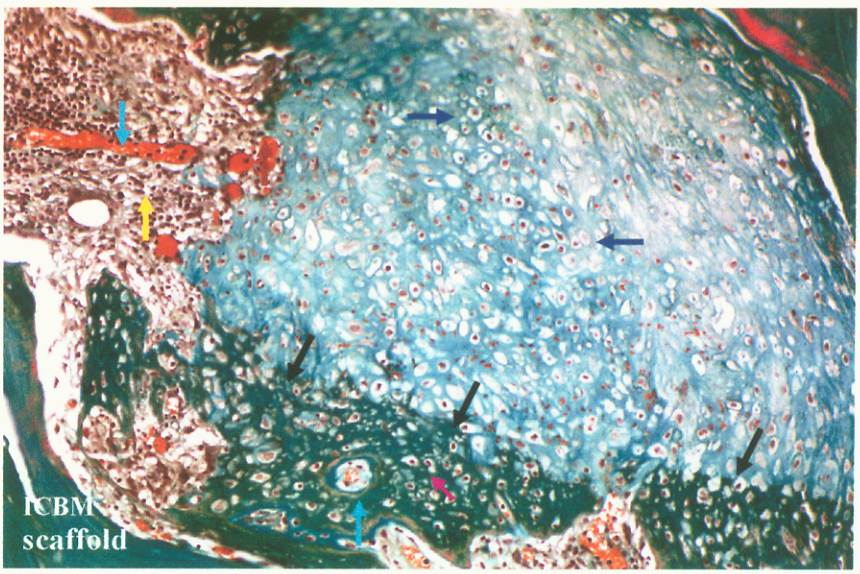

(b) Demonstrating a connecting of cartilage (↑) and mineralized intramembranous bone (↑) with osteocytes in lacunae (↑), blood vessels (↑), bone marrow cells (↑) (Masson Trichrome staining, x 200)

Figure 3-25 (continue): Implantation of fresh bone marrow on the ICBM scaffold at implantation-day 45

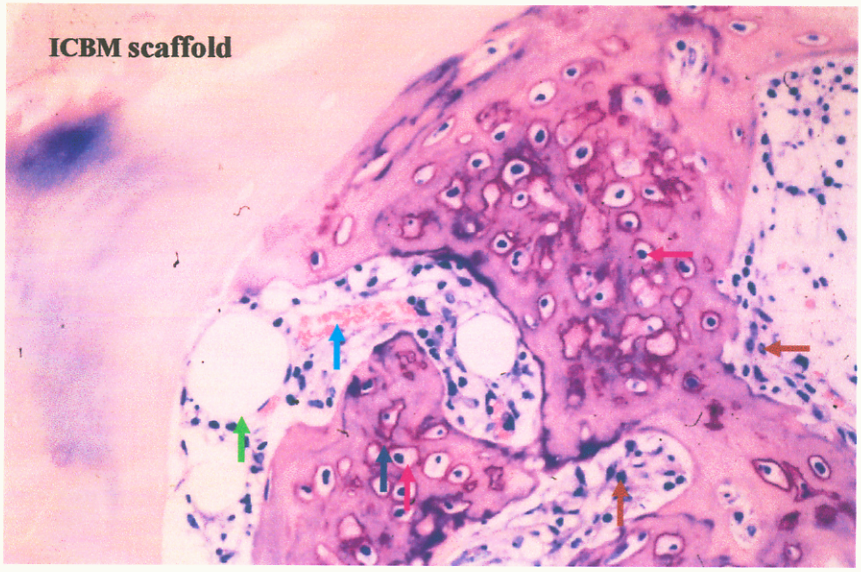

(c) Demonstrating intramembranous bone formation, osteocytes in lacunae (↑), blood vessels (↑) and fat cells (↑) in differentiated bone marrow cells (↑) (Giemsa staining, x 400)

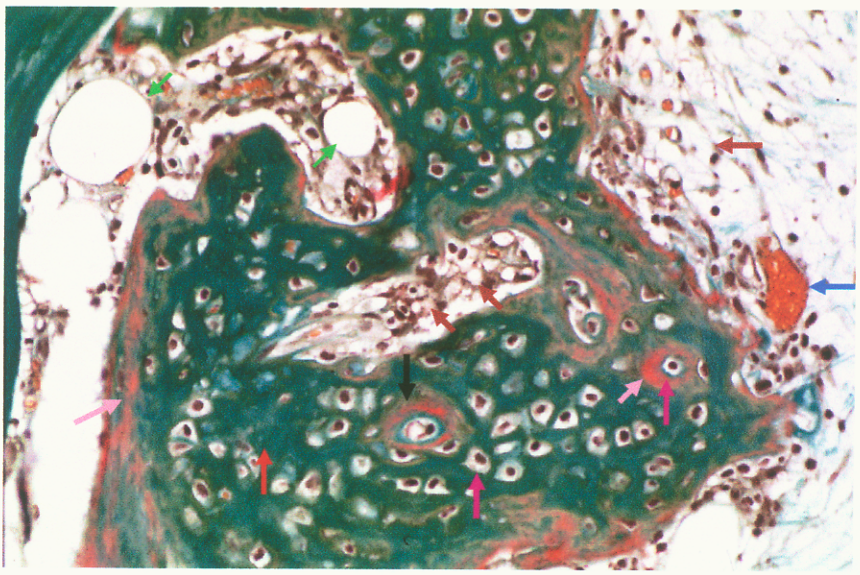

(d) Demonstrating mineralized bone matrix (↑), osteoid (↑), osteocytes (↑), blood vessel (↑) and fat cells (↑) in differentiated bone marrow (↑), observing ossification center (concentric of osteoid around osteocytes) (↑) (Masson Trichrome staining, x 400)

Part II: Effects of PRP on growth and differentiation of premature osteoblasts and mesenchymal stem cells in rat bone marrow

1. Platelet-rich plasma (PRP) preparation

1.1. Concentration of platelets in PRP

The concentration of platelets in PRP was 8.96 ± 0.60 times higher than the concentration in whole blood (Figure 3-26). A high concentration of platelets in PRP was also demonstrated in a PRP smear (Figure 3-27). Average concentrations of platelets ($6.63 \pm 0.23 \times 10^6$ platelets / μl), white blood cells (WBC) ($7.1 \pm 0.36 \times 10^3$ cells / μl) and red blood cells (RBC) ($0.20 \pm 0.09 \times 10^6$ cells / μl) are demonstrated in Table 3-1 and Figure 3-28.

1.2. Preparation efficacy

An average of 8.73±0.28 ml of whole blood was drawn from one rat. This volume of blood yielded PRP 196.55±15.45 μl. According to concentrations of platelets in whole blood and PRP as stated in the previous section, the ratio of platelets in PRP to platelets in whole blood from one rat was 0.201±0.013 or 20.1±1.3 % (Table 3- 2). Therefore, when 40 μl of PRP was added on each scaffold in the PRP 100% group, approximately 5% of the total platelets in one rat were applied on one scaffold (Table 3-3).

2. Concentration of TGF-β1 in PRP

The amount of TGF-β1 was measured from a pool of blood from three experimental days as stated in the Material and Method section. An average concentration of TGF-β1 was 386.416 ± 81.34 ng/ml (Figure 3-29). An average of 14.71 ± 2.02 ng of TGF-β1 was estimated to be released from 2.5×10^8 platelets added on each scaffold in 100% PRP groups of *in vitro* and *in vivo* studies. This would create a concentration of 9.81 ± 1.46 ng / ml TGF-β1 in each well with 1.5 ml of culture medium

in a 100% PRP group cell culture. The amount and concentration of TGF-β1 released on the ICBM scaffold in each group are demonstrated in Table 3- 3 and Figure 3-30.

Figure 3- 26 Concentrations of platelets in whole blood and PRP

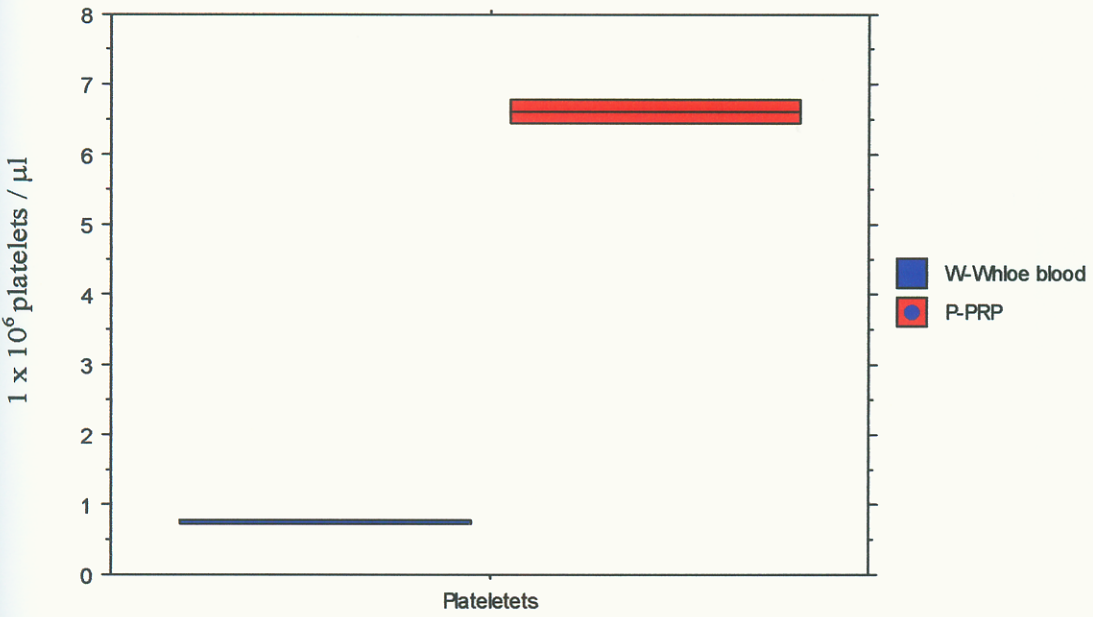

Figure 3- 27 Blood smear of whole blood and PRP

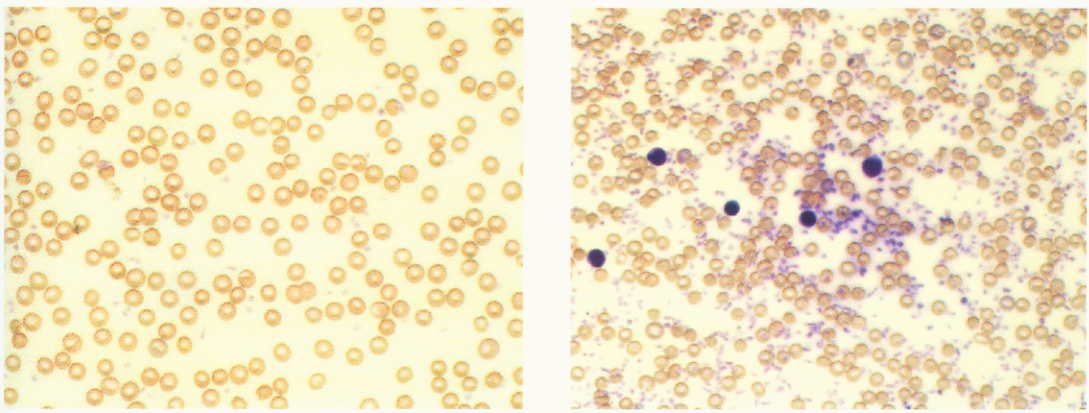

(a) Whole blood (40 x 10 x1) (b) PRP (40 x 10 x1)

Observing blue colour small size particles of platletes, large brown cells with no nucleus of red blood cells and large blue cells of lymphocytes

Figure 3- 28 Average concentrations of red blood cells ($1x10^6$ cells/μl) and white blood cells ($1x10^3$ cells/μl) in whole blood and PRP

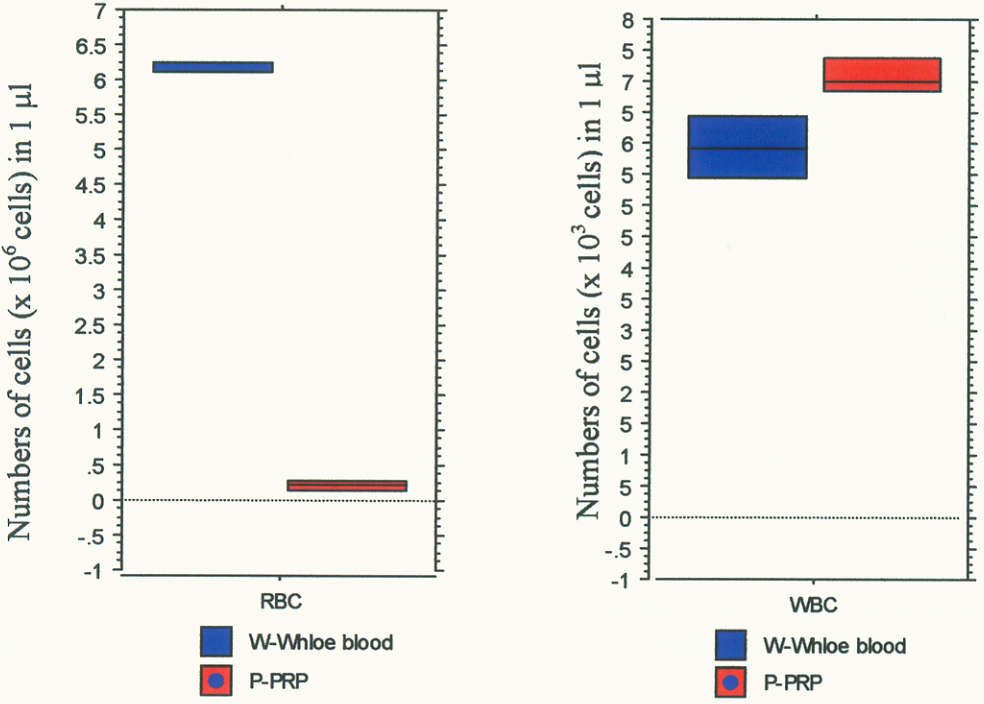

(a) Red blood cells (RBC)

(b) White blood cells (WBC)

Figure 3- 29 Concentration of TGF- β1 (ng/ml) in PRP

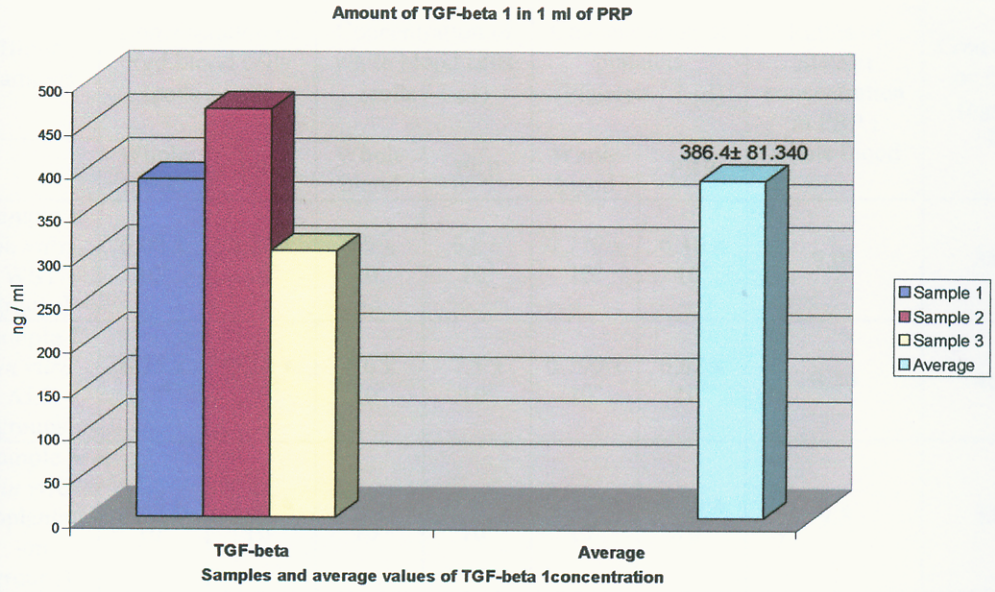

Figure 3- 30 Estimated average amount TGF-β1 applied on each scaffold and concentrations of TGF-β1 in culture medium in each well of 24 well plate

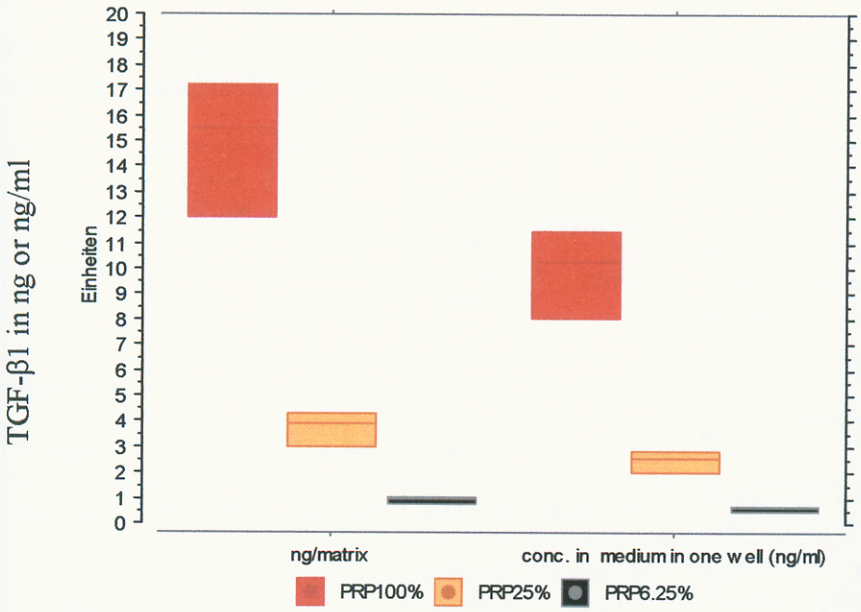

Table 3- 1 Concentration of TGF-β1 (ng/ml) in PRP (ng/ml)

Blood samples	Concentration of Red blood cells (cells / 1 μl)		Concentration of white blood cells (cells / 1 μl)		Concentration of platelets (Platelets / 1 μl)		Ratios of platelet concentration in PRP : whole blood	Concentration of TGF-β1 (ng/ml) in PRP
	Whole blood	PRP	Whole blood	PRP	Whole blood	PRP		
Sample 1 (*in vitro* WST groups)	6.08×10^6	0.22×10^6	5.9×10^3	6.8×10^3	0.710×10^6	6.40×10^6	9.01	386.57
Sample 2 (*in vitro* ALP groups	6.25×10^6	0.10×10^6	6.6×10^3	7.5×10^3	0.799×10^6	6.62×10^6	8.30	467.68
Sample 3 (*in vivo* implantati -on groups)	6.26×10^6	0.28×10^6	5.3×10^3	7.0×10^3	0.725×10^6	6.86×10^6	9.5	304.96
Averages	$6.20 \pm 0.10 \times 10^6$	$0.20 \pm 0.09 \times 10^6$	$5.33 \pm 0.55 \times 10^3$	$7.1 \pm 0.36 \times 10^3$	$0.745 \pm 0.48 \times 10^6$	$6.63 \pm 0.23 \times 10^6$	8.96 ± 0.60	386.416 ± 81.34

Table 3- 2 Efficacy of PRP preparation and ratios of numbers of platelets in PRP to numbers of platelets in whole blood

Blood samples	Volume of whole blood from one rat (μl)	Volume of PRP from one rat (μl)	Platelets in 1 μl of whole blood	Platelets in 1 μl of PRP	Total platelets in whlood blood from one rat	Total platelets in PRP from one rat	Ratios of platelets in PRP / Whole blood
Sample 1	8.5×10^3	207.500	0.7×10^6	6.4×10^6	6.03×10^9	1.32×10^9	0.220 (22%)
Sample 2	8.4×10^3	178.840	0.8×10^6	6.62×10^6	6.71×10^9	1.18×10^9	0.176 (17.6%)
Sample 3	9.3×10^3	203.300	0.73×10^6	6.86×10^6	6.74×10^9	1.39×10^9	0.207 (20.7%)
Average	$8.73 \times 10^3 \pm 0.284 \times 10^3$	$196.55 \times \pm 15.45$	$0.75 \times 10^6 \pm 0.48 \times 10^6$	$6.63 \times 10^6 \pm 0.23 \times 10^6$	$6.50 \times 10^9 \pm 4.04 \times 10^8$	$1.30 \times 10^9 \pm 1.08 \times 10^8$	0.201 ± 0.013 ($20\% \pm 1.3\%$)

Table 3- 3 Amount and concentration of TGF-β1 applied on each scaffold

Samples	PRP 100% or $2.5x10^8$ platelets			PRP 25% or $0.625x10^8$ platelets			PRP 6.25 % or $0.156x10^8$ platelets		
	Amount of PRP 100%, µl / scaffold	Amount of TGF-β1		Amount of PRP 25%, (µl / scaffold)	Amount of TGF-β1		Amount of PRP 6.25%, µl / scaffold	Amount of TGF-β1	
		ng /scaffold	ng / ml of culture medium		ng /scaffold	ng / ml of culture medium		ng /scaffold	ng / ml of culture medium
Sample 1	40	15.460	10.307	20	3.865	2.577	5	.966	0.644
Sample 2	38	17.770	11.847	19	4.442	2.962	5	1.111	0.740
Sample 3	40	10.900	7.267	20	2.725	1.817	5	.681	0.454
Average amount of TGF-β1 (ng)	39.33 ± 0.67	14.71 ± 2.02	9.81 ± 1.46	19.67 ± 0.33	3.68 ± 0.51	2.45 ± 1.35	5 ± 0	0.92 ± 0.13	0.61 ± 0.08

3. Effects of PRP in three-dimensional cell culture, an *in vitro* study

3.1. Expression of osteoblatic marker mRNAs of bone marrow cells

Bone marrow at culture-days 7-8 were pooled and seeded on a 3x5 mm ICBM scaffold for cell culture. At 24 hours after cell seeding the bone marrow cells cultivated in a mineralized medium supplemented with 20 nM dexamethasone and expressed ALP, BMP-2 and type I collagen mRNAs. Expression of osteocalcin mRNA was not found (Figure 3-31)

Figure 3- 31 mRNA expressions of bone marrow cells at 8 day after cell seeding

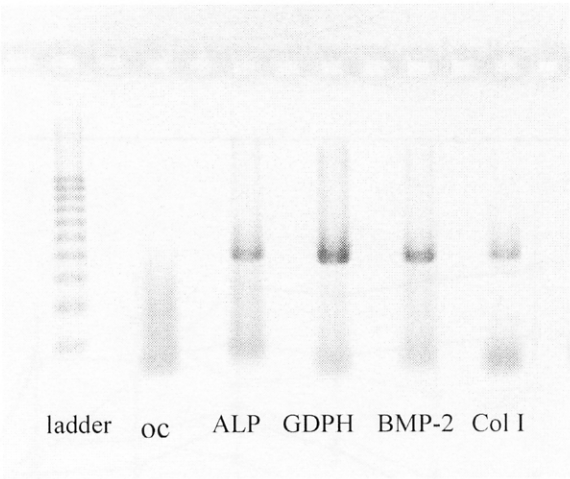

(Ladder=base pair marker, oc=osteocalcin, ALP=alkaline phosphatase, GDPH=house keeping gene, Col I=type I collagen)

3.2. Cell proliferation

In all experimental groups, cell proliferation sharply increased during culture-days 3 – 6 ($p<0.01$), then their growth rate decreased and became relatively stable. Except in the PRP 100% group that proliferation rate was still continuously increasing to the 12th culture-day ($P<0.05$). During culture-days 3-6, PPP and Dexamethasone groups had the

highest proliferation rate and at culture-day 6, these two groups had the highest level of cell proliferation (Figure 3-32).

During the 12^{th} – 21^{st} culture-day, proliferations of cells were stable. Groups of study can be categorised into groups of high and low proliferation rate groups. PRP 100%, Dexamethasone and PPP groups were in a high proliferation rate group, and PRP 25%, PRP 6.25% and BMP-2 groups were in a low proliferation rate group ($p<0.05$). PRP100% had the highest level of cell proliferation followed by Dexamethasone, PPP, 25% PRP, 6.25% PRP and BMP-2 groups, respectively. Cell proliferation was not found in all negative control groups. Optical density of the WST agent of control groups was abruptly decreased to level zero at the 6^{th} culture-day (Figure 3-32).

Figure 3- 32 Proliferation of cells in three-dimensional cell culture

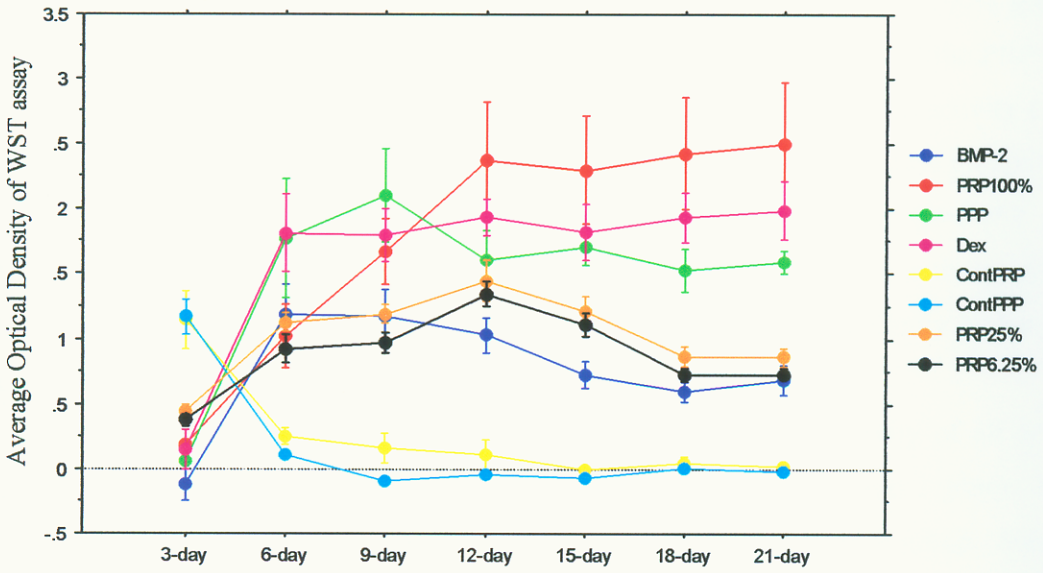

3.3. ALP activity

During the 3^{rd}-9^{th} culture-day, ALP activities of all groups steadily increased ($p<0.01$). The BMP-2 group had the highest rate and level of ALP activity. In contrast, PRP 100% group had the lowest rate and level of ALP activity. The level and increasing rate of the ALP activity of the PPP group was a similar level and rate to the levels and rates of PRP 25% and PRP 6.25% groups ($p>0.05$). ALP activities of Dexamethasone and PRP 100% ($p<0.01$) and PPP groups ($p<0.05$) continuously increased until culture-day 12 and reached their highest level at this point in time. The ALP activity of the other groups, BMP-2, PRP 25% and PRP 6.25% groups reached highest levels at culture-day 9. After reaching the highest level, the ALP of all groups became stable and started to decline.

At the 12^{th} culture-day, the BMP-.2 group had the highest level of ALP activity followed by PPP, PRP 25%v and PRP 6.25%, Dexamethasone and PRP 100% groups. ALP actictivities of PPP was not significantly higher than the activities of the PRP 25% and PRP 6.25% groups ($p>0.05$), but it was significantly higher than the activity of the Dexamethasone group ($p<0.01$). The activities of PRP 25% and PRP 6.25% groups were not significantly higher than the activity of the Dexamethasone group ($p>0.05$). The activity of the Dexamehtasone group was significantly higher than the activity of PRP 100% group ($p<0.01$). ALP activity of the BMP-2 group was significantly higher than the activities of Dexamethasone and PRP 100% group ($p<0.01$).

It can be seen that during the 9^{th}-12^{th} culture-days ALP activity of all groups reached the highest levels. Levels of the activity can be categorized into 3 groups, high, medium and low activity. A group in a high level category was BMP-2 group. Medium level groups included PPP, PRP 25%, PRP 6.25% and Dexamethasone groups. A low level of activity was demonstrated by the PRP 100% group.

After the 12^{th} culture-day levels of ALP activity of all groups became stable and started to decline, except activity of the PRP 100% group. ALP activity of the PRP 100% group was continuously increasing until the 18^{th} culture-day. During the 12^{th} – 18^{th} culture-days ALP activity of PPP groups were significantly higher than the activity of

Dexamethasone group ($p<0.01$), but they were not significantly different from the activity of the PRP 25% and PRP 6.25% groups. ALP activity of BMP-2 group was sharply decreased during 12 – 18 culture-days ($p<0.01$).

At culture-day 21, the ALP activity of each group was in the middle level. It was higher than the level at culture days 3-6 but lower than the level at culture-days 9-12. This was true except for the activity in the PRP 100% group which was in a stable and highest level. The ranges of differences of ALP activities among the groups of study were limited (Figure 3-33). It can be noticed that during culture-days 12 -21, the order of the levels of ALP activity from high to low levels were in an reverse order from the order of WST levels from high to low during the same culture period (Figure 3-32).

Figure 3- 33 ALP acitivity in three-dimensional cell culture

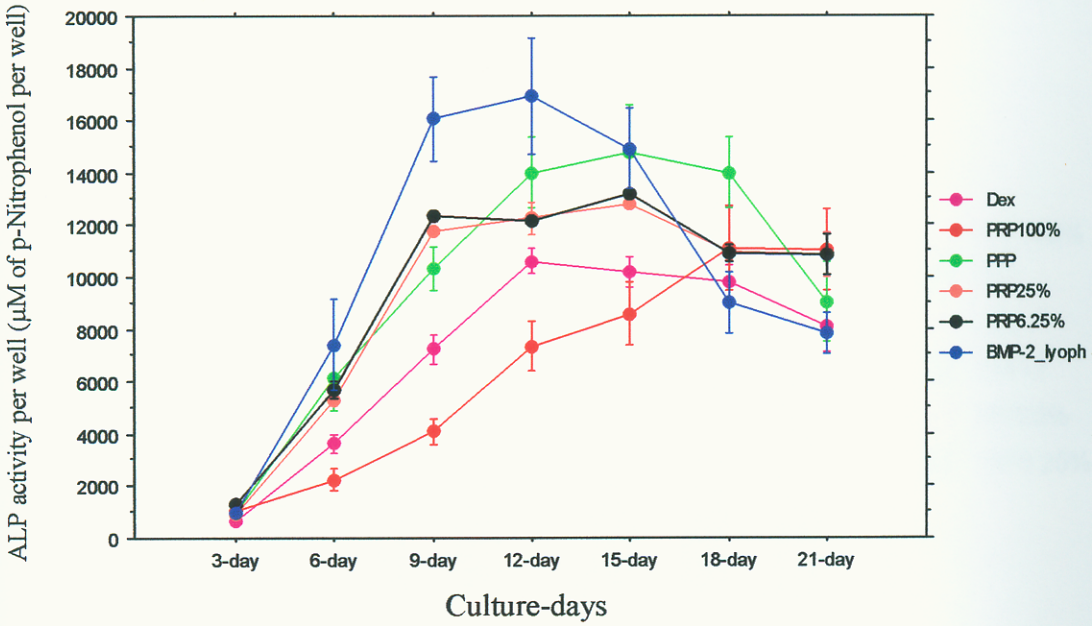

3.4. Calcium contents

The levels of calcium content at the 18th and 21st culture-days were demonstrated. At culture-days 18 and 21 BMP-2 had the highest calcium concentration followed by calcium concentrations in PPP, PRP 25% and 6.25%, PRP 100% and dexamethasone groups, respectively. Calcium concentration in BMP-2, PPP and PRP 25% and 6.25% groups were markedly higher than the concentration in PRP 100% and dexamethasone groups ($P<0.01$). Levels of calcium content of each group at culture-days 18 and 21 were not significantly different ($p>0.05$) (Figure 3-34). It can be noticed that the order of levels of calcium content from high to low levels were similar to the order of ALP levels at culture-day 12 (Figure 3-33).

Figure 3- 34 Calcium contents in three-dimensional cell culture at culture-days 18 and 21

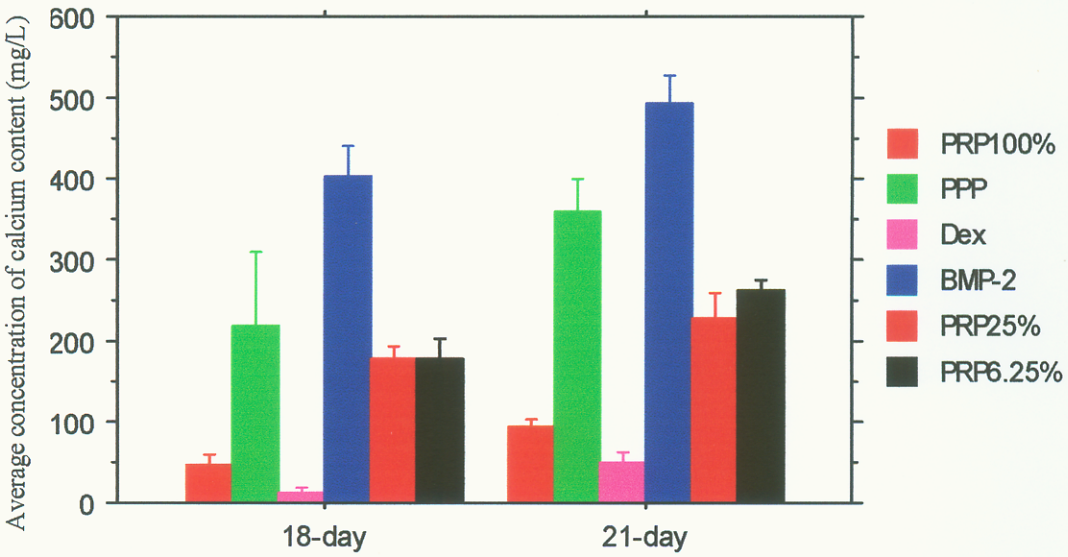

3.5. Morphology of cells on scaffolds, attachment and proliferation of cells on surface of scaffolds

3.5.1. Neutral red staining

It is clearly demonstrated that cells attached, grew and differentiated on the surface of ICBM scaffolds. Cells were found growing on fibrin network of PPP and PRP, which formed a clotting gel covering all surfaces of scaffolds (Figure 3-35 and Figure 3-36).

3.5.2. ALP staining

Most of the cells were fibroblast-like cells and demonstrated positive alkaline phosphatase staining with various intensities. The differences in intensities of positive staining were not measured. Morphologies of cells in each group were slightly different in appearance. The numbers of cells and density of the staining increased with culture time. Growth and differentiation of cells on fibrin network could be seen in BMP-2, PRP 100% and PPP groups (Figures 3-37c, 39c and 40c). Bone marrow cells in every group attached and grew well on ICBM scaffolds (Figures 3-37 – 42).

Figure 3- 35 Neutral red staining of cells growing on an ICBM scaffold and on a fibrin network of Group A: 100% PRP at 15th culture-day

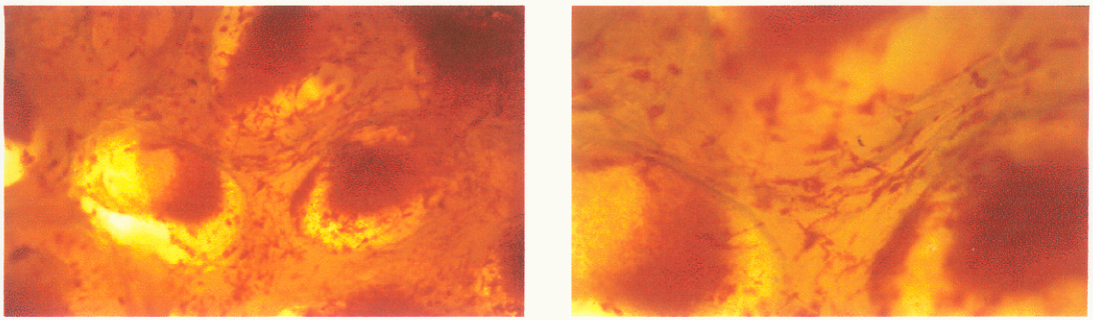

(a) x 200 (b) x 400

Figure 3- 36 Neutral red staining of cells on an ICBM scaffold and on a fibrin network of Group D: PPP at culture-day 15

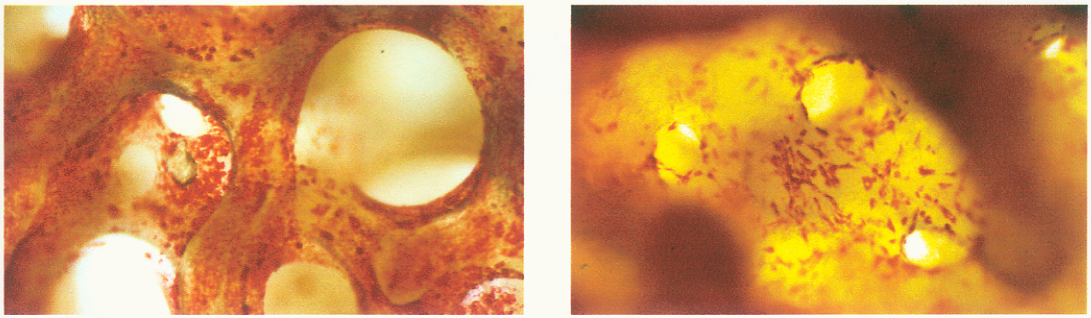

(a) x 200 (b) x 400

Figure 3- 37 Alkaline phosphatase staining of cells Group A: 100%PRP during culture-days 15 – 21

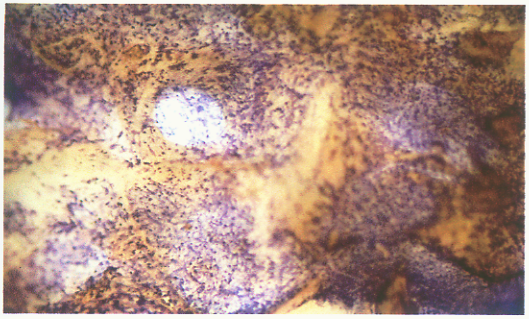

(a) x 100

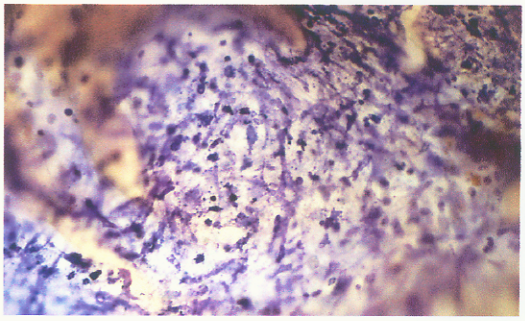

(b) x 200

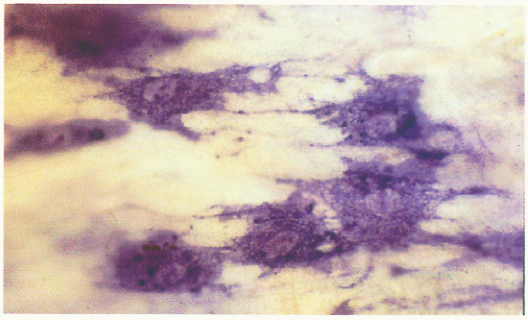

(c) x 600

Figure 3- 38 Alkaline phosphatase staining of cells Group B: PRP 25% during culture-days 15 – 21.

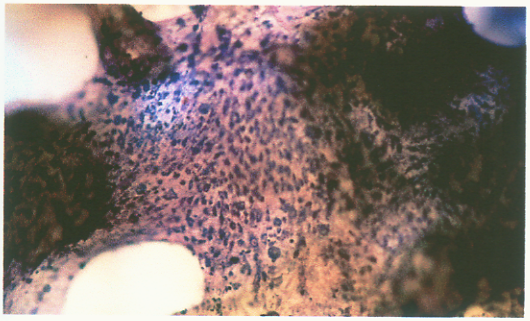

(a) x 100

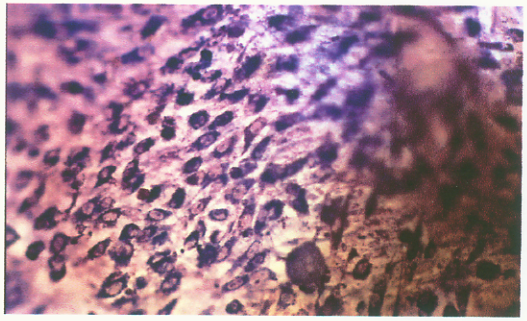

(b) x 200

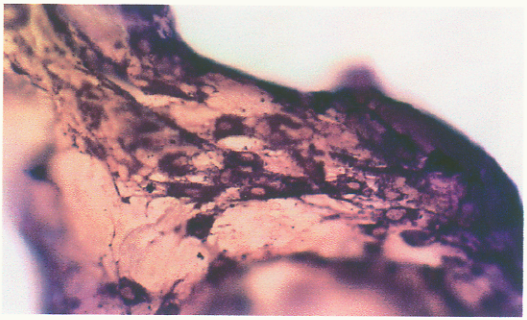

(c) x 400

Figure 3- 39 Alkaline phosphatase staining of cells Group C: PRP 6.25% during culture-days 15 – 21.

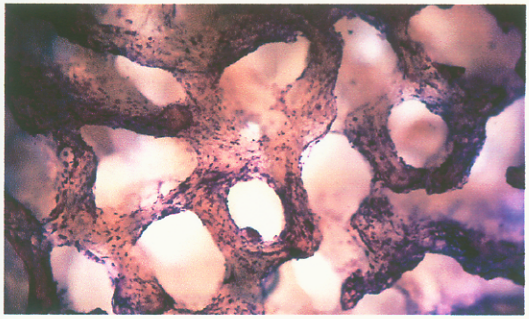

(a) x 100

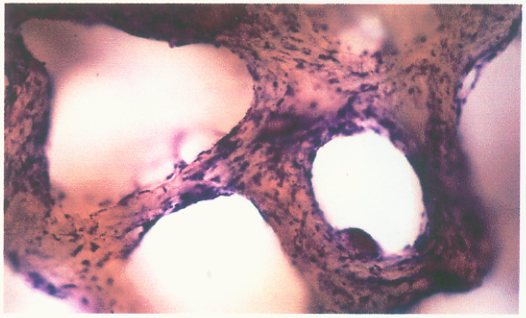

(b) x 200

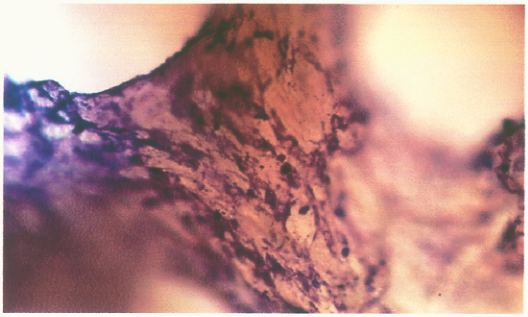

(c) x 400

Figure 3- 40 Alkaline phosphatase staining of cells Group D: PPP during culture-days 15 – 21.

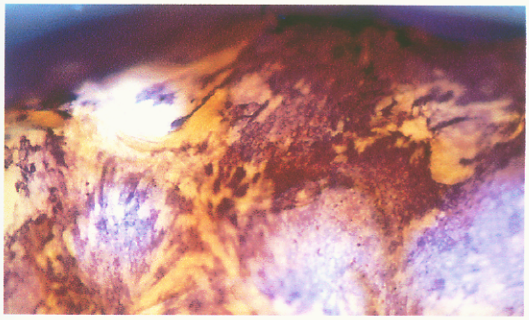

(a) x 200

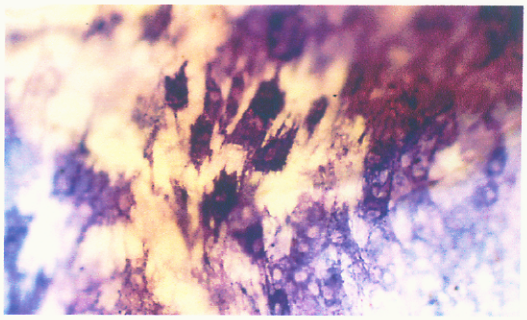

(b) x 400

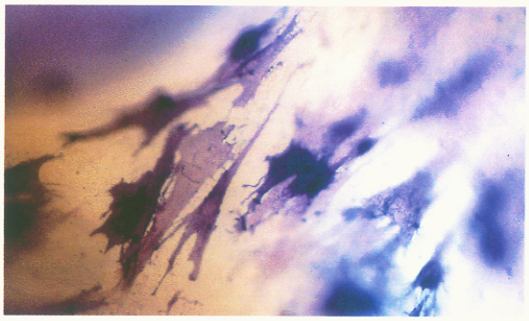

(c) x 600

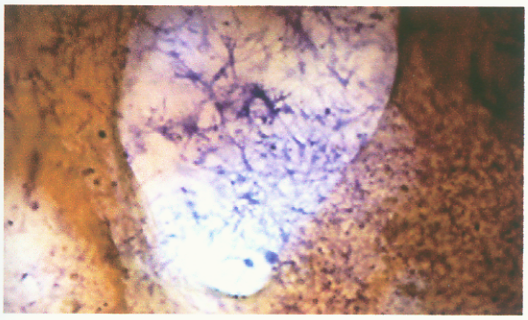

(d) x 200

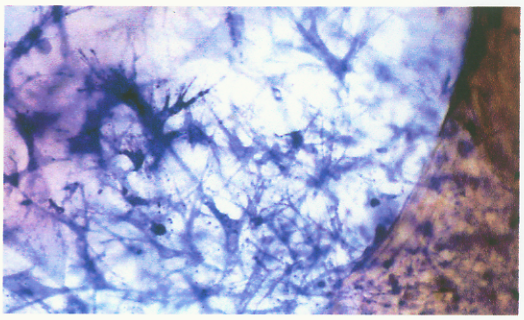

(e) x 400

Figures 40 d and e: demonstrating growth and differentiation of cells on a fibrin net wrapping around ICBM scaffolds

Figure 3- 41 Alkaline phosphatase staining of cells Group E: 300 ng rhBMP-2 during culture-days 15 – 21.

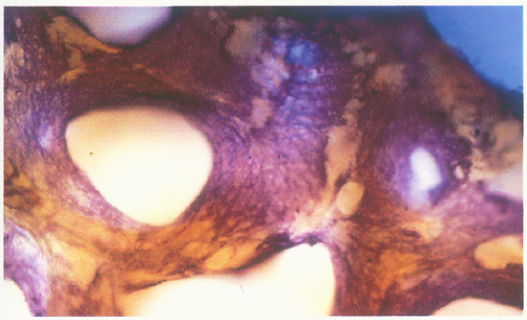

(a) x 100

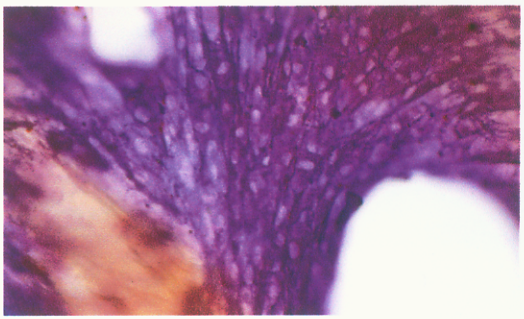

(b) x 400

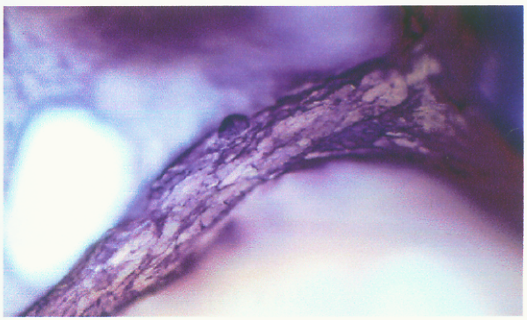

(c) x 400

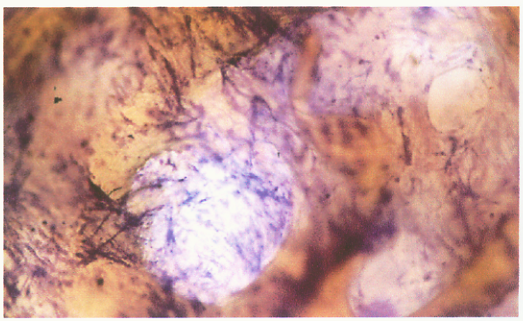

(d) x 200

Demonstrating attachment and osteoblastic differentiation of cells on a structure of ICBM scaffold and on a fibrin network

Figure 3- 42 Alkaline phosphatase staining of cells Group F: Cells without growth factor during culture-days 15 – 21.

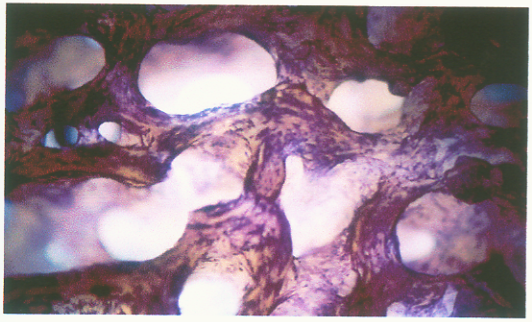

(a) x 100

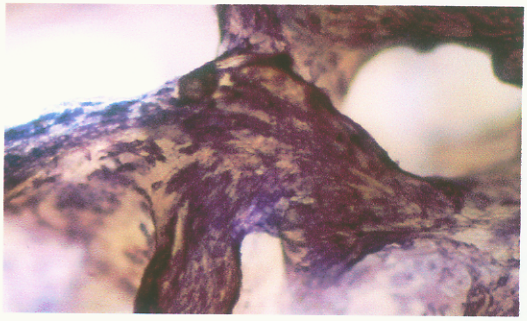

(b) x 200

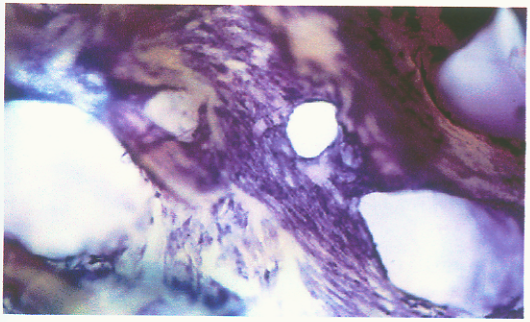

(c) x 400

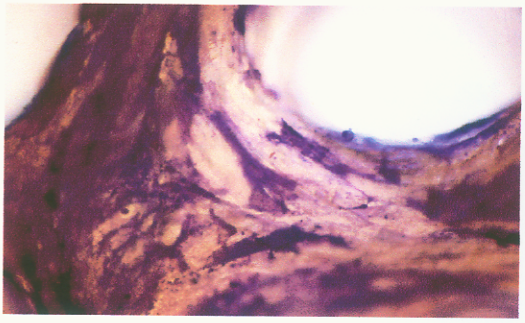

(d) x 600

4. An implantation of bone marrow in nude mice, an *in vivo* study

All mice survived surgical procedures and were sacrificed at the 28th implantation-day.

4.1. Radiographs

4.1.1. Conventional radiographs

Mineralization areas were found in radiographs of all implantation groups, except radiographs of the negative control group. Radiographs of the negative control group (ICBM scaffold only) were radiolucent (Figure 3-45).

The highest mineralization area was found in Group E: ICBM and BMP-2 10 μg (56.20±13.31), followed by Group D: ICBM, bone marrow and BMP-2 1 μg (36.47±5.13), Group F: ICBM and BMP-2 3 μg (28.48±4.65), Group G: ICBM and BMP-2 1 μg (23.42±1.61), Group A: ICBM, bone marrow and whole blood (18.41±6.34), Group C: ICBM, bone marrow and PPP (13.94±4.21), and Group B: ICBM, bone marrow and PRP 100% (7.68±2.03), respectively (Table 3- 4 and Figure 3-43).

The mineralization area of Group E (10 μg BMP-2) was significantly higher than mineralization of other groups ($p<0.001$). Although, the mineralization area of Group D (bone marrow and 1 μg BMP-2) was higher than the areas of Groups F (3 μg BMP-2) and G (1 μg BMP-2), the analysis failed to show any significant differences ($p>0.05$). The mineralization was significantly higher than the areas of Group B (bone marrow and PPP) ($p<0.001$) and Group C (bone marrow and PRP) ($p<0.01$), respectively ($p<0.01$). Group C (bone marrow and PRP 100%) had the lowest mineralization area (Figures 3-44-47).

Table 3- 4 Mineralization areas of each implantation group (sorting by size of mineralization areas)

Categories	Groups of study	Mineralizat-ion areas (mm^2)	Standard error of mean (SE)
Group E	BMP-2 10 µg	56.21	1.63
Group D	BMP-2 1 µg with bone marrow	36.47	5.12
Group F	BMP-2 3 µg	28.48	4.65
Group G	BMP-2 1 µg	23.42	1.61
Group A	Bone marrow with whole blood	18.41	6.04
Group C	Bone marrow with PPP	13.94	4.21
Group B	Bone marrow with PRP 100%	7.68	2.03

Figure 3- 43 Demonstrating mean and standard error of mean of mineralization areas of each implantation group (mean ± SE)

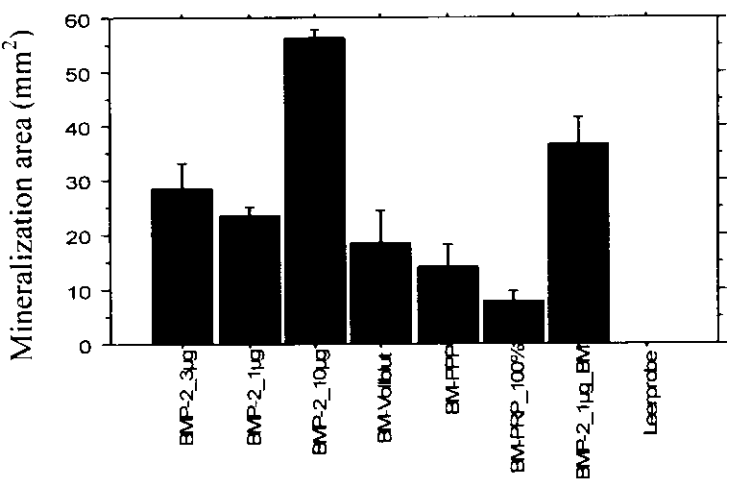

Figure 3- 44 Radiograph of Control group (an implantation of ICBM scaffold only)

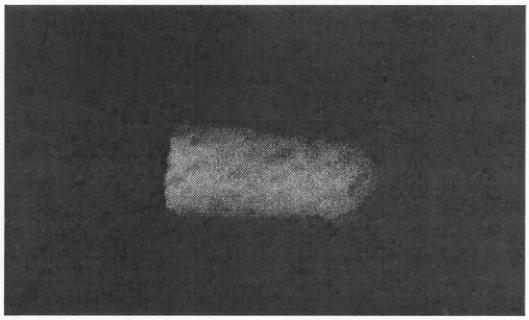

Figure 3- 45 Radiographs of Experimental group I: Bone marrow and blood products

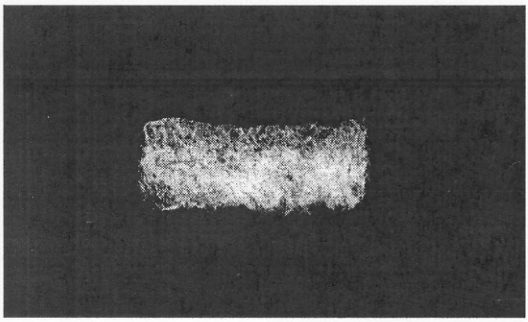

(a) Group A: ICBM, bone marrow and whole blood

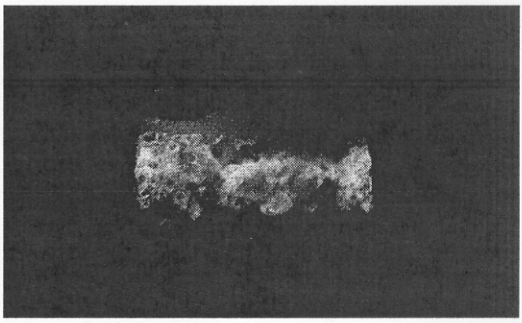

(b) Group B: ICBM, bone marrow and PPP

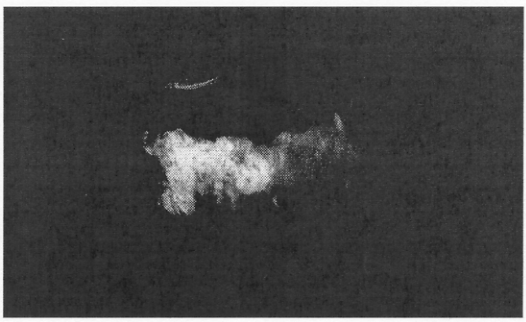

(c) Group C: ICBM, bone marrow and PRP 100%

Figure 3- 46 Radiographs of Experimental group II: Bone marrow and rhBMP-2 1 µg

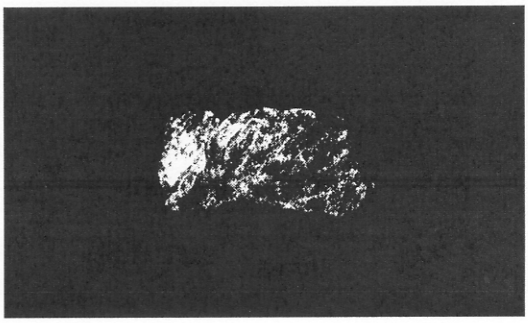

(a) Group D: ICBM, bone marrow and BMP-2 1 µg

Figure 3- 47 Radiographs of Experimental group III: rhBMP-2

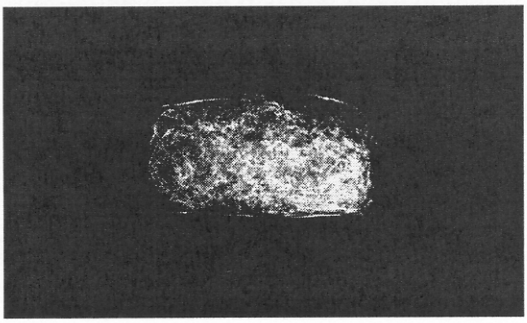

(a) Group E: ICBM and rhBMP-2 10 µg

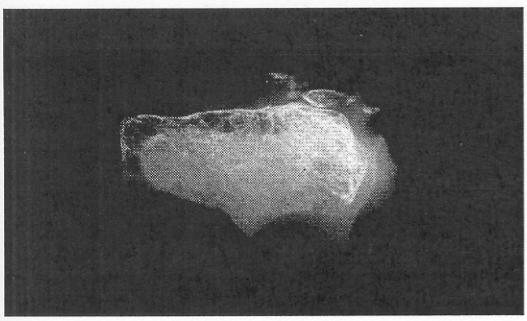

(b) Group F: ICBM and rhBMP-2 3 µg

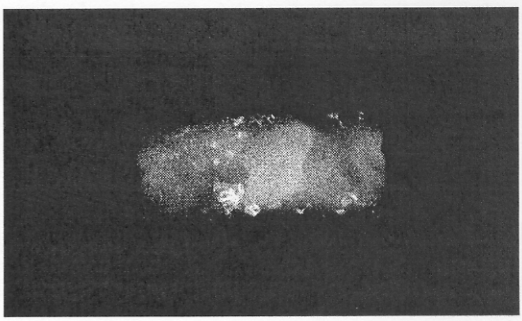

(c) Group G: ICBM and rhBMP-2 1 µg

4.2. Histology of an implantation of bone marrow in nude mice, and *in vivo* study

4.2.1. Control group: ICBM scaffold only

There was no evidence of new bone formation and inflammatory reaction. Pores of the scaffold were filled with loose connective tissue. The ICBM scaffold frame work is a collagenous tissue framework with empty lacunae (Figure 48).

4.2.2. Experimental group I: Bone marrow and blood products

New bone formation was found in pore spaces. The Bone formation pattern in each group was similar. Trabecules of woven bone, osteocytes, osteoblast cell lining, differentiated bone marrow and blood vessels were seen in all groups. Blood and fat cells and blood vessels in differentiated bone marrow were demonstrated. Cartilage formation was found in Groups A (whole blood) and Group C (PRP 100%). At 4 weeks, the structure of the ICBM scaffold was intact. There was no evidence of resorption of the ICBM scaffold.

4.2.2.1. Group A: ICBM, bone marrow and whole blood and Group C: ICBM, bone marrow and PPP

Bone formation in these two groups had a similar pattern and was in the mature stage of bone formation. Trabeculae of mature woven bone with osteocytes in lacunae were found. Most of the bone trabeculae had no osteoblast cell lining and were surrounded by differentiated bone marrow and blood vessels. Osteocalsts and inflammatory reactions of infiltrating polymorphoneuclear leukocytes and lymphocytes were not found (Figures 49-50).

Cartilage formation was found in Group A (Bone marrow and whole blood) but it was not found in the PPP group. Mature chondrocytes with large nuclei embedded in the cartilaginous scaffold were found within pores of the scaffold. Cartilage was rimmed by hyperchromatic cuboidal cells or osteoblasts (Figure 49 c and d).

4.2.2.2. Group B: ICBM, bone marrow and PRP 100%

Intramembranous bone and cartilage formations were found within pores of the ICBM scaffold. Intramembranous bone formation in this group was less mature than bone formation in Group A (bone marrow and whole blood) and Group C (bone marrow and PPP). A larger number of immature bone trabeculae, rimmed with a single layer of osteoblasts, were seen. Bone marrow was less differentiated. Bone trabeculae were surrounded by undifferentiated mesenchymal cells and dense connective tissue stroma (Figure 3-51). This group seemed to have a higher number of undifferentiated cells in connective tissue stroma than what was found in whole blood and PPP groups.

A large area of cartilage formation was found. Mature chondrocytes with large nuclei were embedded in the cartilaginous scaffold. Cartilage was surrounded by a single layer of cuboidal shaped cells which might be osteoblasts (Figure 3-51d).

4.2.3. Experimental group II: ICBM, Bone marrow and BMP-2 1 μg (Group D)

This group demonstrated a combination of patterns for bone formation in terms of ossification areas. New bone formation could be found directly on the surface of an ICBM scaffold and within a pore space.

Trabeculae of mature woven bone with osteocytes embedded in mineralized scaffold were found. Differentiated bone marrow was present. Endochondral ossification was not found (Figure 3-52).

4.2.4. Experimental group III: ICBM and BMP-2 (1- 10 μg)

The pattern of bone formation in each group, Groups E-G, was similar. The amount of new bone formation was different in each group in a dose dependent pattern. Most of the bone trabeculae were mature woven bone without osteoblast cell lining. Differentiated bone marrow, blood cells, fat cells and blood vessels were found infiltrating in pores of ICBM scaffolds surrounding bone trabeculae.

Most of the new bone formation was formed directly on the surface of the ICBM scaffold. A few bone trabeculae were found within pore space and in connective tissue on the periphery of the ICBM scaffold. New bone formation in groups of low dose BMP-2 (1 – 3 μg) was found mostly on peripheral or, outer parts of scaffolds. In Group E: BMP-2 10 μg, new bone was formed both on peripheral and central parts of the ICBM scaffold.

Cartilage formation was not found. There was no sign of inflammation. Histology of implanted BMP-2 10 μg (Group E) was chosen to be representative histologies of this experimental group (Figure 3-53).

Figure 3- 48 Implantation of an ICBM scaffold without cells in the control group

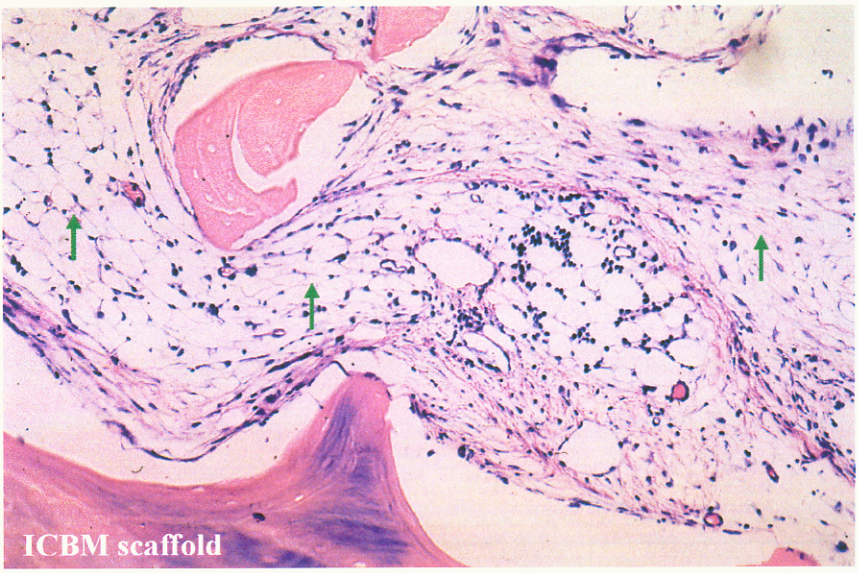

a) Decalcified specimen, demonstrating infiltration of loose connective tissue (↑) within the pore of an ICBM scaffold without an evidence of bone formation or resorption of the scaffold (Giemsa staining, 200)

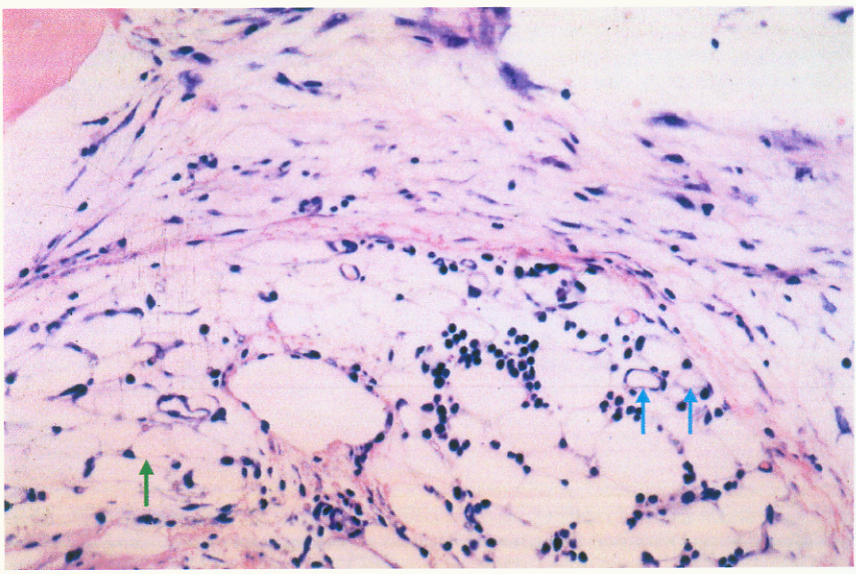

b) Decalcified specimen, demonstrating loose connective tissue (↑) and blood vessles (↑) (Giemsa staining, x 400)

Figure 3- 49 Group A: An implantation of ICBM, bone marrow and whole blood

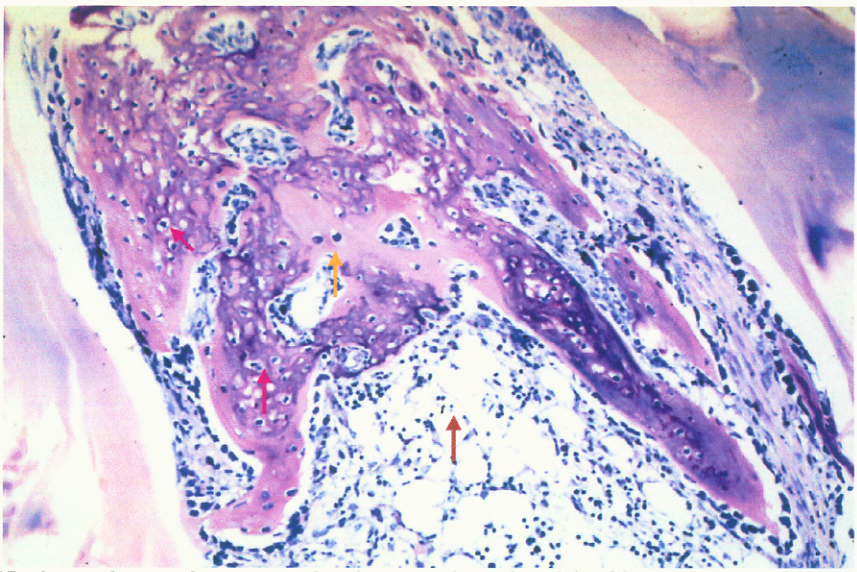

(a) Decalcified specimen, demonstrating bone trabeculae (↑) with osteocytes (↑) in lacunae and bone marrow cells (↑) (Giemsa staining, x 200)

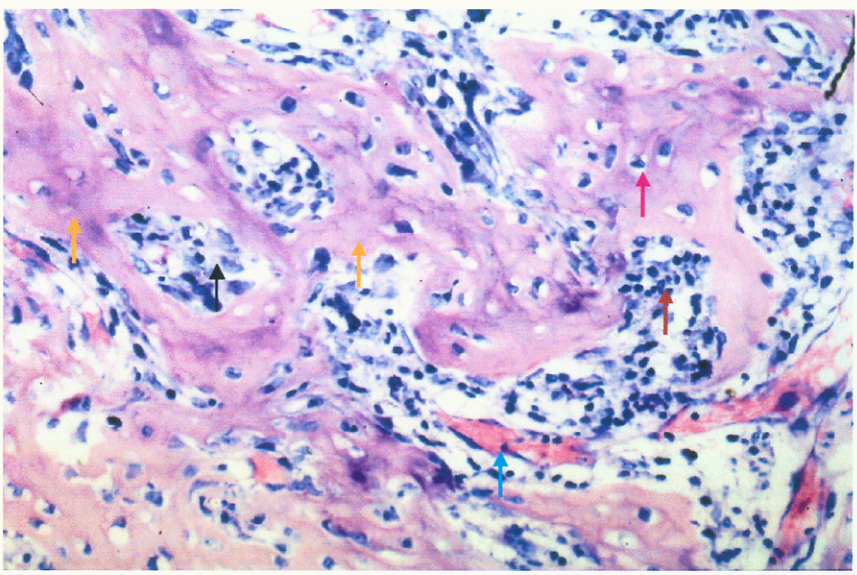

(b) Decalcified specimen, demonstrating trabeculae of mature woven bone (↑), osteocytes (↑), blood vessels (↑) bone marrow cells (↑) and differentiated mesenchymal cells (↑) (Giemsa staining, x 400)

Figure 3-49 (continue): Group A: An implantation of ICBM, bone marrow and whole blood

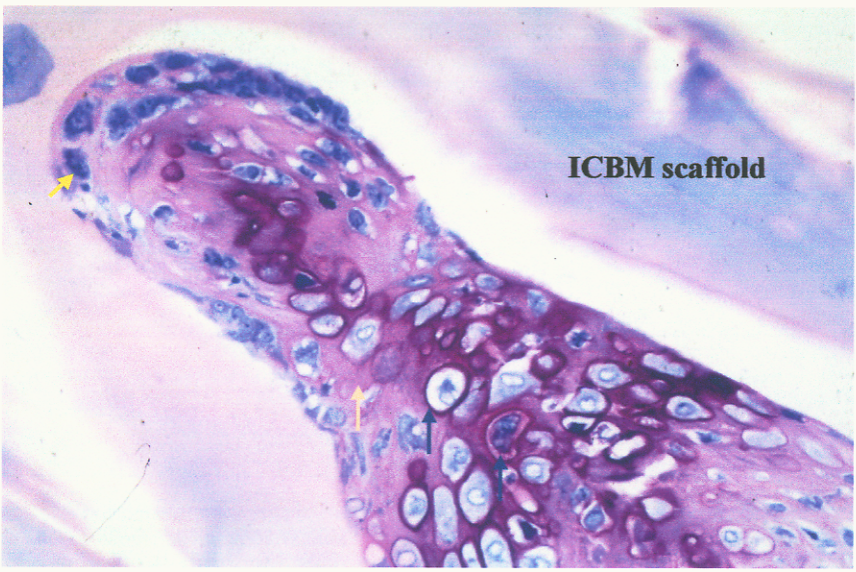

(c) Decalcified specimen, demonstrating cartilage formation observing mature chondrocytes (↑) in the cartilaginous scaffold ( ) and osteoblasts riming (↑) on the border of the cartilage (Giemsa staining, x 400)

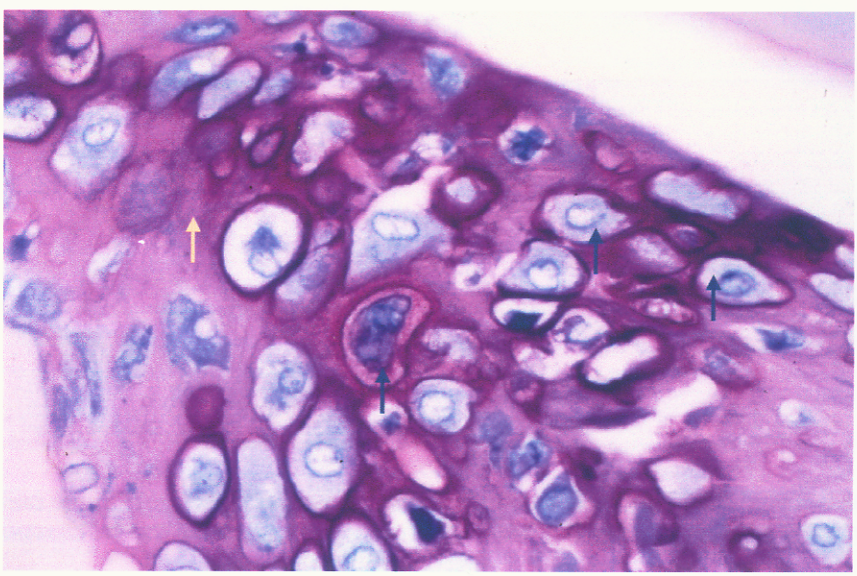

(d) Decalcified specimen, magnification of the central part of the cartilage demonstrating mature chondrocytes with large nuclei (↑) in lacunae embedded in the cartilagenous scaffold ( ) (Giemsa staining, x 800)

Figure 3- 50 Group C: An implantation of ICBM, bone marrow and PPP

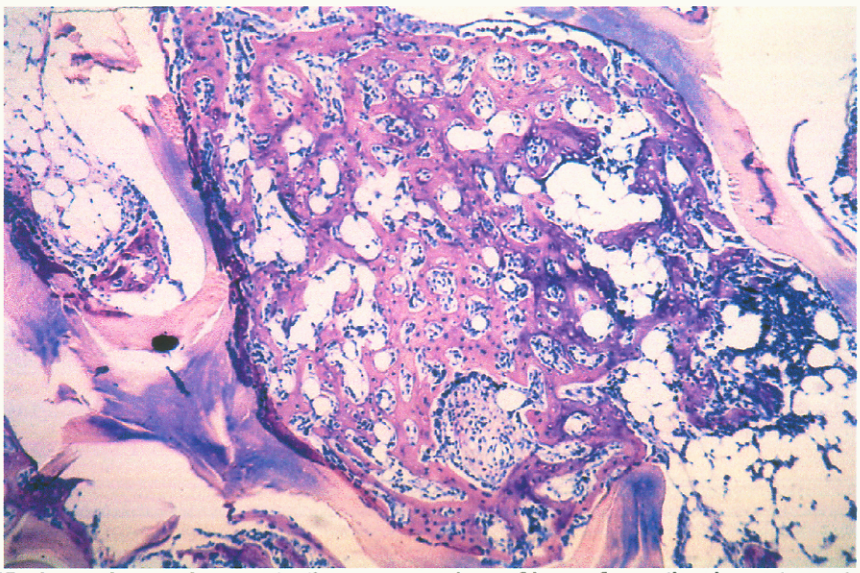

(a) Decalcified specimen, demonstrating an overview of bone formation in mature stage within a pore of the scaffold (Giemsa staining, x 100)

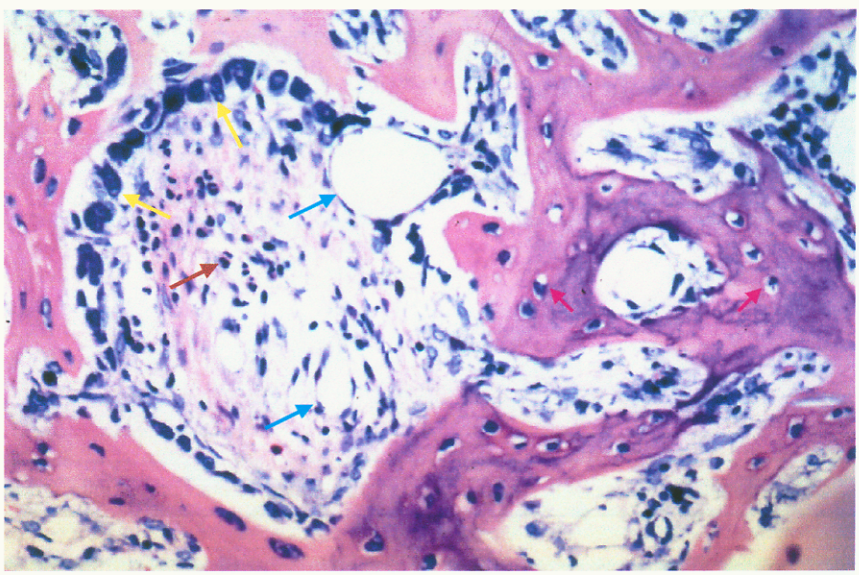

(b) Decalcified specimen, magnification of bone trabeculae demonstrating osteocytes (↑) in small lacunae, osteoblast cell lining (↑), bone marrow (↑) and vascular connective tissue stroma (↑) (Giemsa staining, x 400)

Figure 3-50 (continue): Group C: An implantation of ICBM, bone marrow and PPP

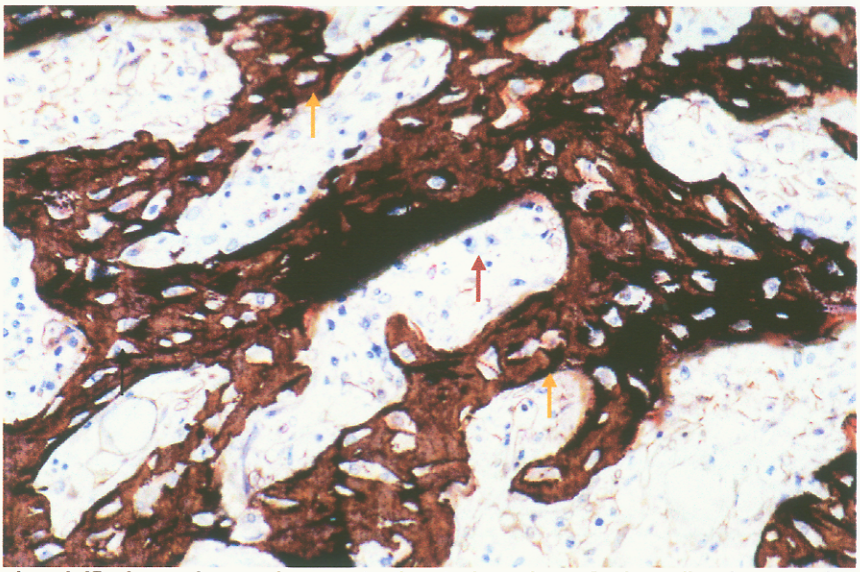

(c) Undecalcified specimen, demonstrating trabeculae of mineralized woven bone (↑), surrounded by bone marrow (↑) (von Kossa and Giemsa double stainings, x 400)

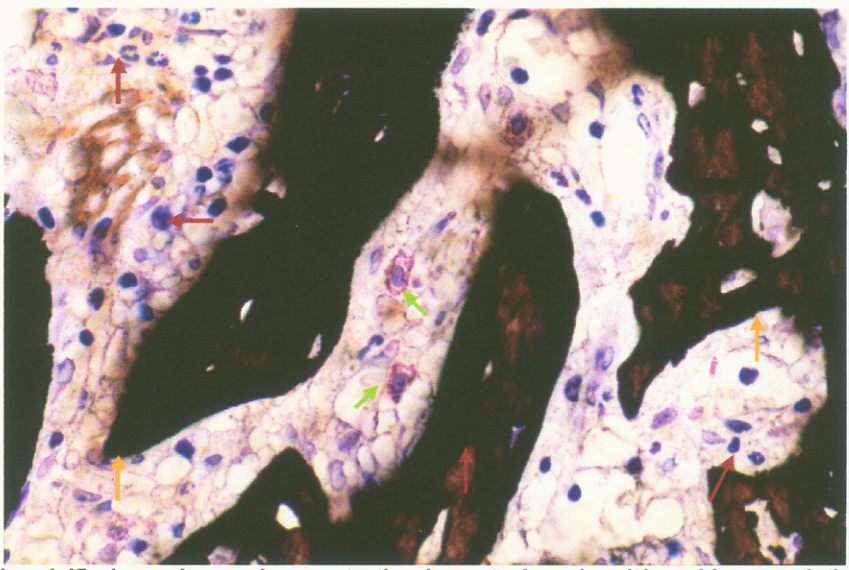

(d) Undecalcified specimen, demonstrating bone trabeculae (↑) and hemopoietic cells in differentiated bone marrow cells (↑), observing plasma cells with granular pink cytoplasm (↑) (von Kossa and Giemsa double stainings, x 400)

Figure 3- 51 Group B: An implantation of ICBM, bone marrow and PRP 100%

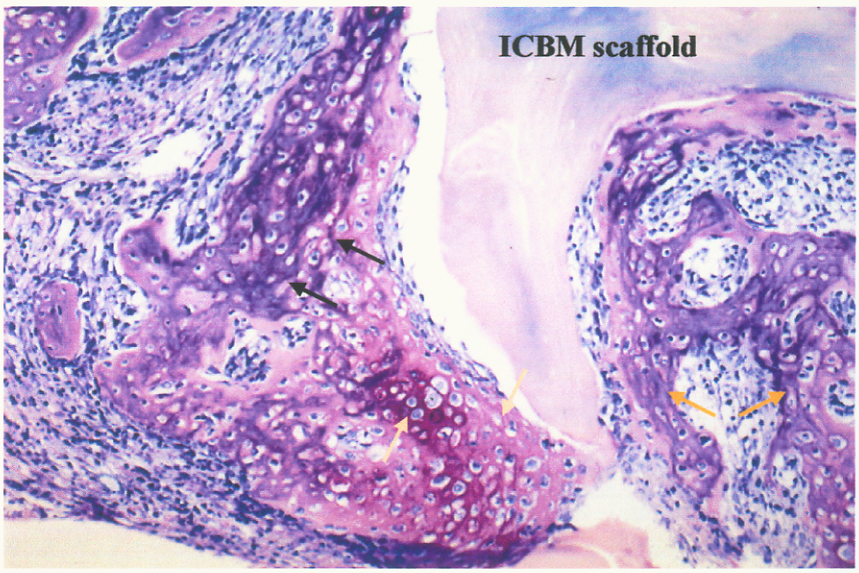

(a) Decalcified specimen, demonstrating endochrondral and intramembranous bone formations, observing bone on outer surface of cartilage (↑), mature cartilage (↑) and mature woven bone (↑) and surrounding dense undifferentiated mesenchymal cells (Giemsa staining, x 200)

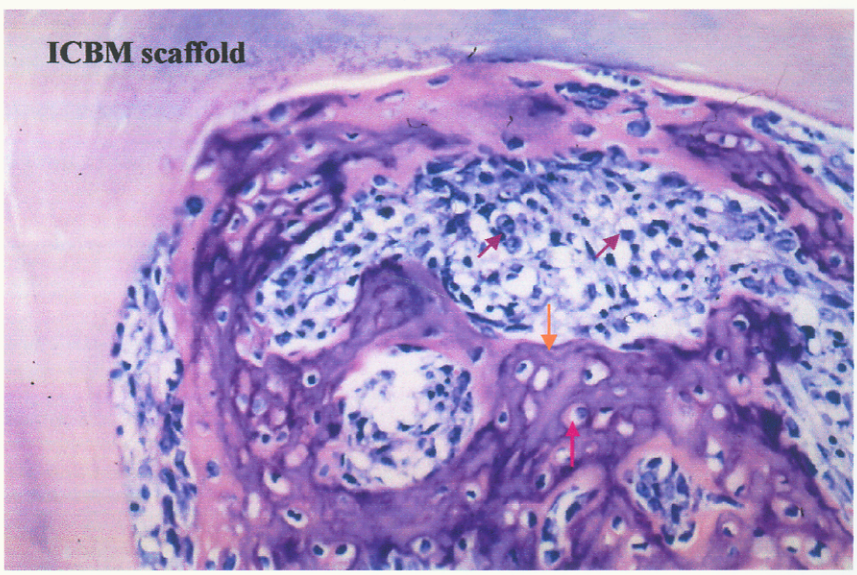

(b) Decalcified specimen, demonstrating trabeculae of mature woven bone (↑), osteocytes in lacunae (↑) without lining layer of osteoblasts, surrounded by cuboidal shaped cells of undifferentiated mesenchymal cells (↑) (Giemsa staining, x 400)

Figure 3-51 (continue): Group B: An implantation of ICBM, bone marrow and PRP

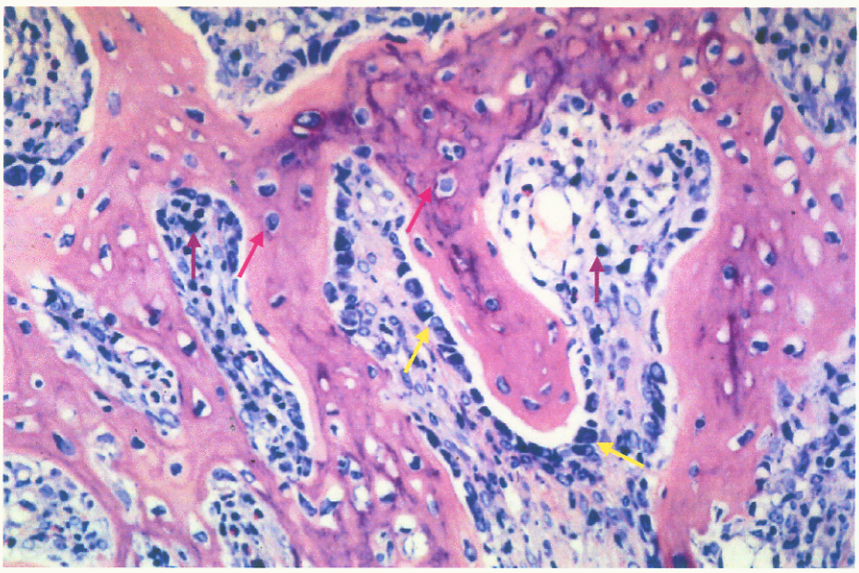

(c) Decalcified specimen, demonstrating immature bone formation, bone trabeculae, osteocytes in large lacunae (↑), Osteoblast cell lining (↑), and undifferentiated cells (↑) (Giemsa staining, x 400)

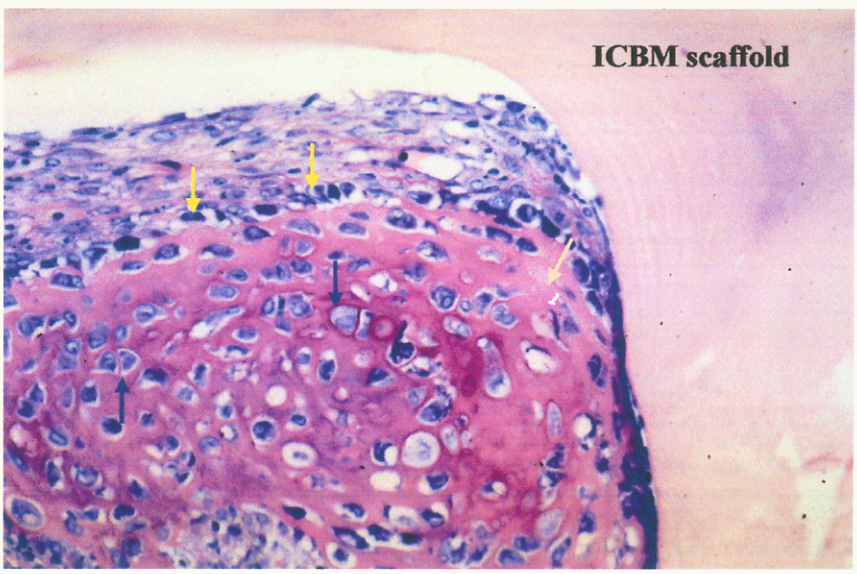

(d) Decalcified specimen, demonstrating cartilage formation observing mature chondrocytes with large nuclei in lacunae embedded in cartilage scaffold and rimming of cartilage with layer of osteoblasts (Giemsa staining, x 400)

Figure 3- 52 Group D: An implantation of ICBM, bone marrow and BMP-2 1 µg

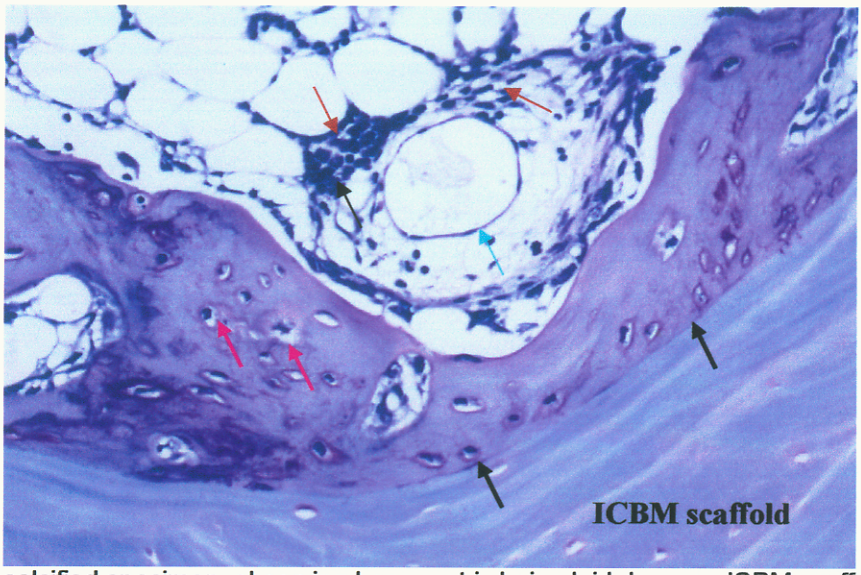

(a) Decalcified specimen, observing bone matrix being laid down on ICBM scaffold (↑), osteocytes (↑), differentiated bone marrow (↑) and blood vessel (↑) (Giemsa staining, x 400)

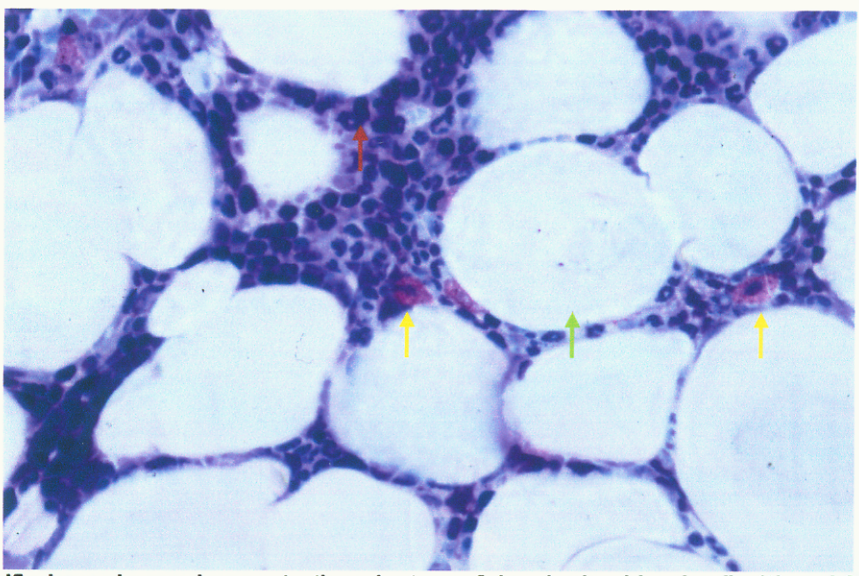

(b) Decalcified specimen, demonstrating clusters of developing blood cells (↑) and fat cells (↑), observing plasma cells with granular pink cytoplasm (↑), in differentiated bone marrow (Giemsa staining, x 600)

Figure 3-52 (continue): Group D: An implantation of ICBM, bone marrow and BMP-2 1 µg

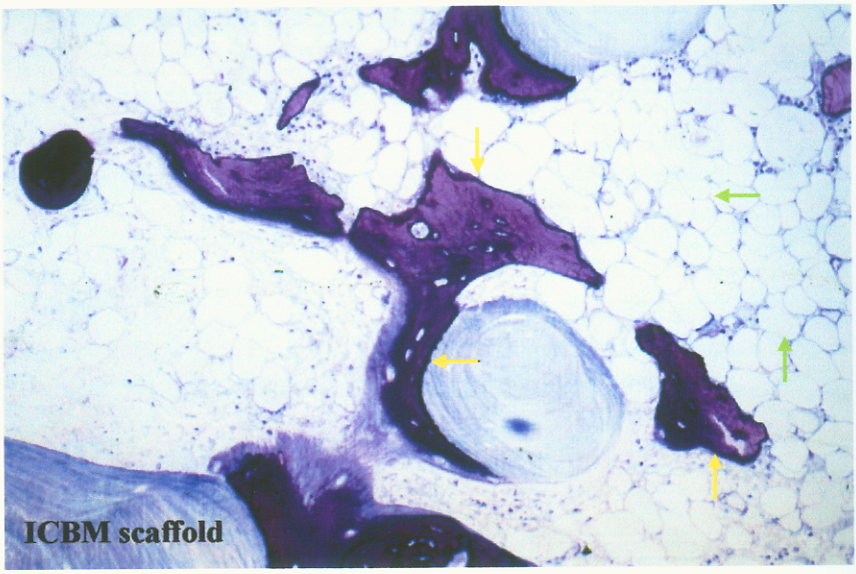

(c) Undecalcified specimen, demonstrating mineralized bone trabeculae within a pore (↑) and on the surface of ICBM scaffold (↑) and bone marrow with large numbers of fat cells (↑) (Toluidine blue staining, x 200)

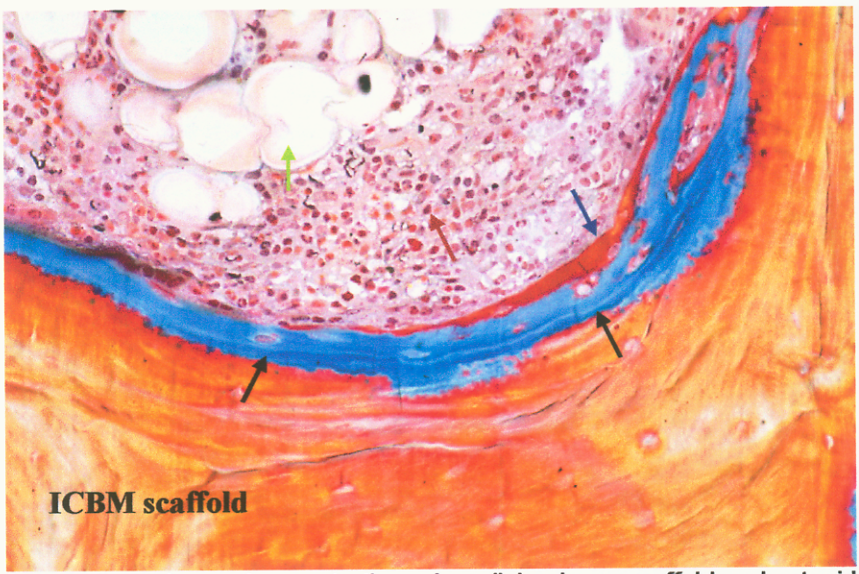

(d) Undecalcified specimen, demonstrating mineralizing bone scaffold and osteoid seam on surface of an ICBM scaffold and blood and fat cells of differentiated bone marrow

Figure 3- 53 Group F: An implantation of ICBM and BMP-2 10 µg

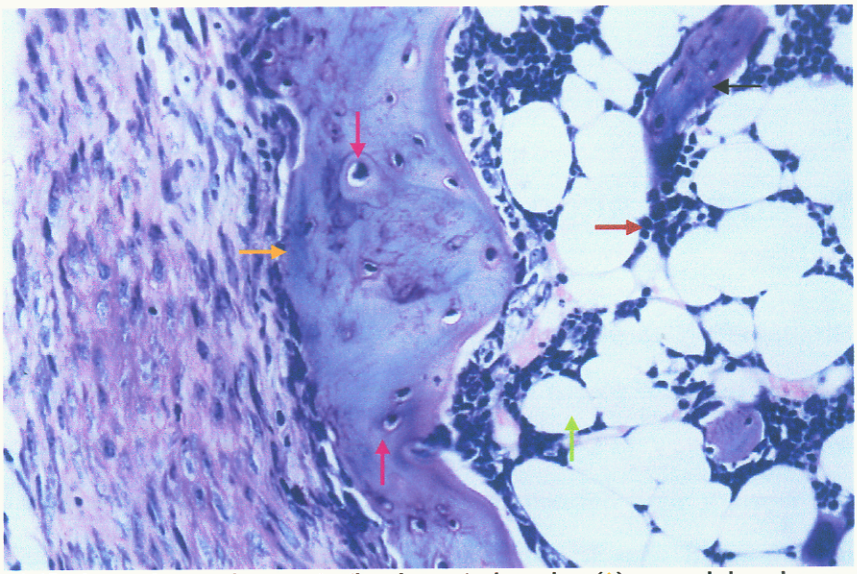

(a) Decalcified specimen, demonstrating bone trabeculae (↑) on peripheral area of ICBM scaffold, osteocytes (↑) and differentiated bone marrow (↑) with a large numbers of fat cells (↑) (Giemsa staining 40 x 10 x 1)

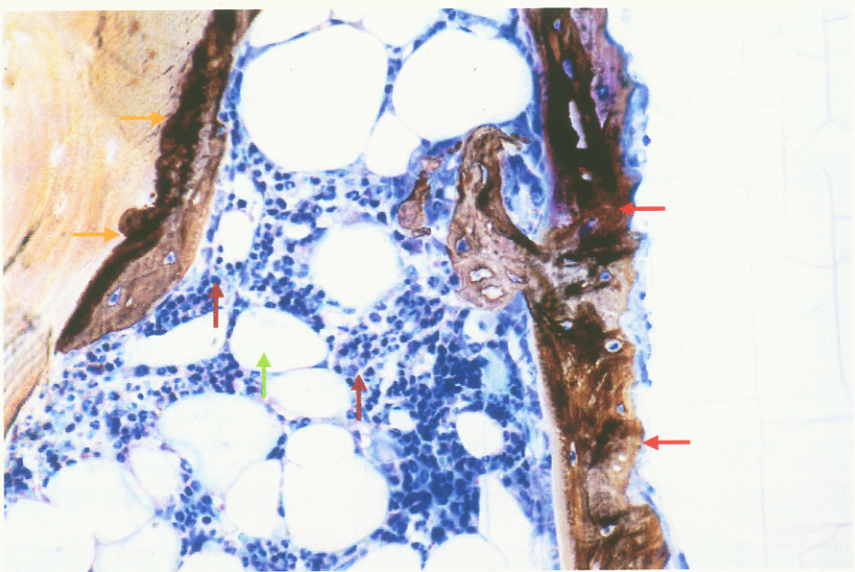

(b) Undecalficified specimen, demonstrating mineralized bone trabeculae on surface (↑) and on peripheral area of ICBM scaffold (↑), and differentiated bone marrow with blood (↑) and fat cells (↑) (von Kossa and Giemsa double staining, x 400)